HHS Public Access

Author manuscript

*Int J Comput Methods*. Author manuscript; available in PMC 2019 February 15.

Published in final edited form as:

*Int J Comput Methods*. 2018 June ; 15(1): . doi:10.1142/S0219876218500287.

# A General Approach to Derive Stress and Elasticity Tensors for Hyperelastic Isotropic and Anisotropic Biomaterials

**Jie Cheng**[*] and **Lucy T. Zhang**[*,†,‡]

[*]Department of Mechanical Aerospace and Nuclear Engineering Rensselaer Polytechnic Institute, Troy, New York 12180, USA

[†]School of Mechanical Engineering, Tianjin University of Science and Technology, Tianjin, P. R. China

## Abstract

Hyperelastic models are of particular interest in modeling biomaterials. In order to implement them, one must derive the stress and elasticity tensors from the given potential energy function explicitly. However, it is often cumbersome to do so because researchers in biomechanics may not be well-exposed to systematic approaches to derive the stress and elasticity tensors as it is vaguely addressed in literature. To resolve this, we present a framework of a general approach to derive the stress and elasticity tensors for hyperelastic models. Throughout the derivation we carefully elaborate the differences between formulas used in the displacement-based formulation and the displacement/pressure mixed formulation. Three hyperelastic models, Mooney–Rivlin, Yeoh and Holzapfel–Gasser–Ogden models that span from first-order to higher order and from isotropic to anisotropic materials, are served as examples. These detailed derivations are validated with numerical experiments that demonstrate excellent agreements with analytical and other computational solutions. Following this framework, one could implement with ease any hyperelastic model as user-defined functions in software packages or develop as an original source code from scratch.

### Keywords

Hyperelastic models; anisotropy; Mooney–Rivlin; Yeoh; Holzapfel–Gasser–Ogden; mixed formulation

## 1. Introduction

Hyperelastic models have been successfully applied to various types of biomaterials scaling from onion epidermis [Qian *et al.* (2010)] to breast tissues [O'Hagen and Samani (2009)], from carotid vessels [Masson *et al.* (2010, 2008); Bols *et al.* (2013)] to breast tumors [Oberai *et al.* (2009)], and a number of animal organs including brain [Karimi *et al.* (2013); Kaster *et al.* (2011); Rashid *et al.* (2013)], lung [Bel-Brunon *et al.* (2014); Rausch *et al.* (2011)], liver and kidney [Fu *et al.* (2013); Untaroiu *et al.* (2015); Umale *et al.* (2013)]. A detailed review

[‡]Corresponding author: zhanglucy@rpi.edu.

of the applications of isotropic hyperelastic models on biological tissues is provided in [Wex *et al.* (2015)]. According to [Steinmann *et al.* (2012)], hyperelastic models can be classified as phenomenological or micro-mechanical. The latter are derived from statistical mechanics arguments on networks of idealized chain molecules while the former utilize more or less complex, frequently polynomial formulations in terms of strain invariants or principle stretches. Because of the popularity of hyperelastic models, many commercial softwares have hyperelastic models as a built-in material selection. For instance, Abaqus FEA and COMSOL offer Mooney–Rivlin model, Yeoh model, Neo–Hookean model, etc. They also allow users to provide subroutines to define new models.

Although hyperelastic models have been frequently used with finite element method to model nonlinear deformation behaviors, it is not straightforward to implement them because of the complicated procedure involved in deriving stress and elasticity tensors. The stress tensor is used to form the equilibrium equation, and the elasticity tensor is the keystone to form the tangent stiffness matrix that is used to solve the equilibrium equation. There are few existing literature or references providing a systematic approach to evaluate stress and elasticity tensors. An indicial method to derive the stress and elasticity tensors for Mooney–Rivlin model is presented in Bower [2009], which in the author's opinion, is not easy to be transplanted to another model. In Belytschko *et al.* [2000], a general method to find the tangent stiffness matrix for any hyperelastic model in index notation is introduced in an abstract form with no illustrated examples. A step-by-step method written in tensor notation is derived in Holzapfel [2000], which we refer to frequently in this paper. But again limited examples for different models are shown and there is no computational results to validate the finite element implementation. Some derivations for specific models can be found in some early publications [Weiss *et al.* (1996); Nicholson (1995)]. A more recent paper [Suchocki (2011)] presents the implementation of Knowles model within Abaqus, using tensor notation described in Holzapfel [2000]. But instead of using the spatial tensor of elasticity, the author used Jaumann objective rate as it is used in Abaqus [2014]. In this paper, we will present a systematic approach to derive the stress and elasticity tensors for any given hyperelastic model.

This paper is motivated to address this obstacle and clarify some of the key concepts presented in the existing literature in this field, as explained earlier. We present a framework for the derivation and walk the readers through the entire process with detailed examples. With the detailed derivation and the neat workflow, readers should be able to quickly implement any hyperelastic model. This is not only useful to the researchers who develop their own finite element code but also to those who work with commercial or open-source software with user-defined functions to include new constitutive models, especially for the ever-increasing newly defined models to describe biomaterials.

The rest of this paper is organized as follows: in Sec. 2, we introduce the basics of the hyperelastic model followed by the general procedures to derive the stress and elasticity tensors. To demonstrate how they can be applied for specific models, we present three different examples: Mooney–Rivlin model, Yeoh model, and Holzapfel–Gasser–Ogden (HGO) model. Mooney–Rivlin model is simple but very effective in modeling large strain nonlinear behavior of incompressible materials such as rubber and biomaterial. Yeoh model

contains only one invariant but with a second-order term. It is not complicated but can correctly predict the behavior of elastomer material in the range of a greater extent of deformation than the Mooney–Rivlin model [Gajewski *et al.* (2015)], and is able to characterize the stiffening phenomenon of vulcanized rubber. The HGO model is designed to model collagen fiber-reinforced biological materials. This anisotropic model is so widely used that many commercial and open-source finite element packages have included it as a standard or user-defined model, such as in Abaqus [2014], COMSOL [2012] and FEBio [Mass *et al.* (2012)]. In Sec. 3, two sets of numerical experiments are presented: biaxial tension and 2D vessel expansion. The experiments are performed using the three hyperelastic models, where the results are validated with analytical solutions and existing computational results whenever possible, and isotropic and anisotropic behaviors are observed and compared. Finally, the conclusions are drawn in Sec. 4.

## 2. Stress and Elasticity Tensors in Hyperelastic Models

In this section, we briefly review the hyperelastic models and their decomposition, and the general approach to derive stress and elasticity tensors, followed by three examples of different models: Mooney–Rivlin model, Yeoh model and HGO model. The first two are isotropic models written as polynomial functions of invariants. There are also isotropic models written as exponential functions or combination of both forms [Fung (1967); Demiray (1972); Veronda and Westmann (1970)]. Yet not all biomaterials are isotropic. For example, the stomach wall tissues in pigs are found to be direction-dependent [Zhao *et al.* (2008)]. Heart muscles have strong directional properties as well [Saraf *et al.* (2007)]. Materials like these are modeled as a combination of a ground substance and one or more families of fibers which are continuously arranged in the ground material. In literature, this kind of materials are referred as transversely isotropic materials. HGO model is one of the anisotropic models with two families of fibers. To model anisotropy, two pseudo-invariants are introduced. However, the procedure of the derivation of the stress and elasticity tensors remain the same for both isotropic and anisotropic materials.

### 2.1. Hyperelastic models

Generally in continuum mechanics we use constitutive equations to describe the stress components in terms of other functions such as strain. This functional relationship distinguishes different types of materials. For hyperelastic material, we postulate there exists a Helmholtz free-energy function $\Psi$, which is defined per unit reference volume. If $\Psi$ is uniquely determined by the deformation tensor $\mathbf{F}$ or other strain tensor, it is called strain–energy function. For example, all isotropic models are functions of the right Cauchy–Green tensor, which is defined as $\mathbf{C} = \mathbf{F}^T\mathbf{F}$. If the strain is given, the stress can be uniquely determined from the strain–energy function. Our discussion will be focused on rubber-like materials as often the case for biomaterials which are modeled as incompressible or nearly incompressible. In this case, the strain–energy function is postulated to have a unique decoupled form:

$$\Psi(\mathbf{C}) = \Psi_{\text{vol}}(J) + \Psi_{\text{iso}}(\overline{\mathbf{C}}), \quad (1)$$

where $\Psi_{vol}(J)$ and $\Psi_{iso}(\bar{\mathbf{C}})$ are volumetric and isochoric responses of the material, respectively. $J$ is the Jacobian or the volume ratio defined as the determinant of the deformation tensor $\mathbf{F}$, and $\bar{\mathbf{C}}$ is the modified right Cauchy–Green tensor defined as $\bar{\mathbf{C}} = J^{-2/3}\mathbf{C}$. Likely the modified counterpart of the deformation is written as $\bar{\mathbf{F}} = J^{-1/3}\mathbf{F}$. The modified tensors are associated with the volume-preserving, because their determinants are 1. The concept of decomposition of the deformation and strain tensors is necessary for the mixed formulation because we need to deal with the volumetric and isotropic parts individually.

In the displacement-based formulation, the volumetric part of the strain-energy function is a penalty to allow for a small compressibility:

$$\Psi_{vol} = \kappa G(J), \quad (2)$$

where $\kappa$ is the penalty parameter and can be interpreted as the bulk modulus, $G(J)$ is the penalty function and may adopt the simple form:

$$G(J) = \frac{1}{2}(J-1)^2. \quad (3)$$

In the displacement/pressure mixed formulation, the volumetric part of the strain-energy function acts as a Lagrange condition to enforce the incompressibility $J - 1 = 0$:

$$\Psi_{vol} = p(J-1), \quad (4)$$

where $p$ is a Lagrange multiplier and can be identified as the hydrostatic pressure. For nearly incompressible materials, $p$ can be determined from the deformation. However, for incompressible materials, it has to be determined from the equilibrium equation and any imposed boundary conditions.

Furthermore, if the material is isotropic, the strain-energy function can be expressed as a function of the three invariants of the right (or left) Cauchy–Green tensor. These invariants are $I_1 = \mathrm{tr}(\mathbf{C}) = \mathrm{tr}(\mathbf{B})$, $I_2 = \frac{1}{2}(I_1^2 - \mathrm{tr}(\mathbf{C}^2)) = \frac{1}{2}(I_1^2 - \mathrm{tr}(\mathbf{B}^2))$, and $I_3 = \det(\mathbf{C}) = \det(\mathbf{B}) = J^2$, where $\mathbf{B}$ is the left Cauchy–Green tensor defined as $\mathbf{B} = \mathbf{F}\mathbf{F}^T$. They also have their modified counterparts: $\bar{I}_1 = J^{-2/3}I_1$, $\bar{I}_2 = J^{-4/3}I_2$, and $\bar{I}_3 = 1$. In fact, most isotropic models can be expressed as:

$$\Psi = \Psi_{vol}(J) + \Psi_{iso}(\bar{I}_1, \bar{I}_2). \quad (5)$$

## 2.2. Stress Evaluation and Elasticity Tensor

Based on the postulation of strain–energy function, it follows that the work done on hyperelastic materials in a dynamic process within a time interval $[t_1, t_2]$ is the difference

between the strain–energy in the two states. It can also be proven that the work can be written as the integration of the tensor product of conjugate stress–strain rate pairs [Holzapfel (2000)]:

$$\Psi(\mathbf{F}_2) - \Psi(\mathbf{F}_1) = \int_{t_1}^{t_2} \mathbf{S}:\dot{\mathbf{E}}dt = \int_{t_1}^{t_2} \mathbf{P}:\dot{\mathbf{F}}dt \quad (6)$$
$$= \int_{t_1}^{t_2} \boldsymbol{\sigma}:\dot{\mathbf{e}}dt,$$

where $\mathbf{P}$ is the first Piola–Kirchhoff (PK1) stress defined as $\mathbf{P} = J\boldsymbol{\sigma}\mathbf{F}^{-T}$, $\mathbf{S}$ is the second Piola–Kirchhoff (PK2) stress tensor, $\mathbf{E}$ is the Green–Lagrange strain tensor defined as $\mathbf{E} = \frac{1}{2}(\mathbf{C} - \mathbf{I})$, and $\mathbf{e}$ is Euler–Almansi strain tensor which is defined as $\mathbf{e} = \frac{1}{2}(\mathbf{I} - \mathbf{F}^{-T}\mathbf{F}^{-1})$.

If the material is homogeneous, the PK2 stress $\mathbf{S}$ can be determined by

$$\mathbf{S} = \frac{\partial \Psi(\mathbf{E})}{\partial \mathbf{E}} = 2\frac{\partial \Psi(\mathbf{C})}{\partial \mathbf{C}}. \quad (7)$$

Similarly, the PK1 stress and Cauchy stress can be determined as $\mathbf{P} = 2\mathbf{F}\frac{\partial \Psi(\mathbf{C})}{\partial \mathbf{C}}$ and $\boldsymbol{\sigma} = J^{-1}\mathbf{F}\frac{\partial \Psi(\mathbf{C})}{\partial \mathbf{C}}\mathbf{F}^T$.

Not surprisingly, the PK2 stress can also be written in a decoupled form with volumetric and isochoric parts:

$$\mathbf{S} = 2\frac{\partial \Psi(\overline{\mathbf{C}})}{\partial \mathbf{C}} = \mathbf{S}_{\text{vol}} + \mathbf{S}_{\text{iso}}, \quad (8a)$$

$$\mathbf{S}_{\text{vol}} = 2\frac{\partial \Psi_{\text{vol}}(J)}{\partial \mathbf{C}} = Jp\mathbf{C}^{-1} = J^{1/3}\rho\overline{\mathbf{C}}^{-1}, \quad (8b)$$

$$\mathbf{S}_{\text{iso}} = 2\frac{\partial \Psi_{\text{iso}}(\overline{\mathbf{C}})}{\partial \mathbf{C}} = J^{-2/3}\mathbb{P}:\overline{\mathbf{S}}, \quad (8c)$$

where $\bar{\mathbf{S}}$ is the fictitious PK2 stress defined as $\bar{\mathbf{S}} = 2\partial\Psi_{\text{iso}}(\bar{\mathbf{C}})/\partial\bar{\mathbf{C}}$ and $\mathbb{P}$ is the projection tensor defined as $\mathbb{P} = \mathbb{I} - \frac{1}{3}\mathbf{C}^{-1} \otimes \mathbf{C} = \mathbb{I} - \frac{1}{3}\overline{\mathbf{C}}^{-1} \otimes \overline{\mathbf{C}}$ in which $\otimes$ is the dyadic multiplication symbol and $\mathbb{I}$ is the fourth-order identity tensor, i.e., $\mathbb{P}_{ijkl} = \frac{1}{2}(\delta_{ik}\delta_{jl} + \delta_{il}\delta_{jk}) - \frac{1}{3}\overline{C}^{-1}{}_{ij}\overline{C}_{kl}$.

Note that if the material is completely incompressible, the hydrostatic pressure $p$ is independent from the displacement $\mathbf{u}$; otherwise $p$ can be determined from the displacement even when it is treated as an independent variable by:

$$p = \frac{d\Psi_{\text{vol}}(J)}{dJ} = \kappa \frac{dG(J)}{dJ}. \quad (9)$$

For the material that is not completely incompressible, either displacement-based formulation or mixed formulation can be used. If we explicitly substitute $p$ with Eq. (9), we end up with a displacement-based formulation as $\mathbf{u}$ is the only unknown to be solved; if we leave $p$ as an unknown and use Eq. (9) as a relaxed constraint in the Lagrangian multiplier method, we will have a displacement/pressure mixed formulation.

The solutions in nonlinear finite element methods are often obtained incrementally with Newton's method. The elasticity tensors is crucial in the implementation of Newton's method. In the material description or the reference configuration, the elasticity tensor $\mathbb{C}$ is defined as the gradient of the PK2 stress to its work conjugate strain, the Green–Lagrange strain:

$$\mathbb{C} = \frac{\partial \mathbf{S}(\mathbf{E})}{\partial \mathbf{E}} = 2\frac{\partial \mathbf{S}(\mathbf{C})}{\partial \mathbf{C}} = 4\frac{\partial^2 \Psi(\mathbf{C})}{\partial \mathbf{C}\,\partial \mathbf{C}}. \quad (10)$$

Similar to $\Psi$ and $\mathbf{S}$, the elasticity tensor can also be rewritten in the decoupled form:

$$\mathbb{C} = 2\frac{\partial \mathbf{S}}{\partial \mathbf{C}} = \mathbb{C}_{\text{vol}} + \mathbb{C}_{\text{iso}}, \quad (11a)$$

$$\begin{aligned} \mathbb{C}_{\text{vol}} &= 2\frac{\partial \mathbf{S}_{\text{vol}}}{\partial \mathbf{C}} \\ &= J^{-1/3}\tilde{p}\overline{\mathbf{C}}^{-1} \otimes \overline{\mathbf{C}}^{-1} - 2J^{-1/3}p\overline{\mathbf{C}}^{-1} \odot \overline{\mathbf{C}}^{-1}, \end{aligned} \quad (11b)$$

$$\begin{aligned} \mathbb{C}_{\text{iso}} &= 2\frac{\partial \mathbf{S}_{\text{iso}}}{\partial \mathbf{C}} \\ &= \mathbb{P} : \overline{\mathbb{C}} : \mathbb{P}^T + \frac{2}{3}\text{Tr}(J^{-2/3}\overline{\mathbf{S}})\widetilde{\mathbb{P}} - \frac{2}{3}J^{-2/3}(\overline{\mathbf{C}}^{-1} \otimes \mathbf{S}_{\text{iso}} + \mathbf{S}_{\text{iso}} \otimes \overline{\mathbf{C}}^{-1}), \end{aligned} \quad (11c)$$

where $\tilde{p}$ is defined as $\tilde{p} = p + Jdp/dJ$. Note that in the mixed formulation $\tilde{p} = p$ because $p$ is independent of $J$. $\odot$ is an operator defined as the derivative of the inverse of a second-order tensor with respect to itself, i.e., $\bar{\mathbf{C}}^{-1} \odot \bar{\mathbf{C}}^{-1} = -\partial \bar{\mathbf{C}}^{-1}/\partial \bar{\mathbf{C}}$; $\bar{\mathbb{C}}$ is the fourth-order fictitious

elasticity tensor defined as $\overline{\mathbb{C}} = 2J^{-2/3}\frac{\partial \overline{\mathbf{S}}}{\partial \overline{\mathbf{C}}} = 4J^{-4/3}\frac{\partial^2 \Psi_{\text{iso}}(\overline{\mathbf{C}})}{\partial \overline{\mathbf{C}}\partial \overline{\mathbf{C}}}$; Tr(●) is the trace defined as $\text{Tr}(\bullet) = (\bullet) : \mathbf{C}$; and $\tilde{\mathbb{P}}$ is the modified projection tensor of fourth-order defined as $\tilde{\mathbb{P}} = \mathbf{C}^{-1} \odot \mathbf{C}^{-1} - \frac{1}{3}\mathbf{C}^{-1} \otimes \mathbf{C}^{-1} = J^{-4/3}(\overline{\mathbf{C}}^{-1} \odot \overline{\mathbf{C}}^{-1} - \frac{1}{3}\overline{\mathbf{C}}^{-1} \otimes \overline{\mathbf{C}}^{-1})$.

Therefore, once the stress expressions $\mathbf{S}_{\text{vol}}$ and $\mathbf{S}_{\text{iso}}$ are obtained, we can evaluate the elasticity tensor $\mathbb{C}$ by substituting Eq. (8) into Eq. (11). The stress and elasticity tensors in the current configuration can be obtained easily using push-forward operations as derived in Appendix A.

Note that in some models the strain-energy is written as functions of principal stretches $\lambda_1$, $\lambda_2$, $\lambda_3$ instead of deformation invariants, for example Ogden [1972] and Li *et al.* [2016]. In other compressible models, the strain–energy function is not decoupled into volumetric and isochoric parts such as the compressible Neo-Hookean model in Holzapfel [2000]. In those cases, the same framework can still be applied where Eqs. (7) and (10) are unchanged. However, Eqs. (8) and (11) cannot no longer be used directly as they are derived using the decoupled form. Instead, the derivatives in Eqs. (7) and (10) have to be calculated via the corresponding variables: $\lambda_i$ or $I_i$ ($i = 1, 2, 3$).

### 2.3. Examples

**2.3.1. Mooney–Rivlin model—**Originally derived by Mooney [1940] and Rivlin [1948], Mooney–Rivlin model is a polynomial function of $\bar{I}_1$ and $\bar{I}_2$. The first-order Mooney–Rivlin is the most widely used to model biological tissues because of its simplicity. However it was found that the first-order Mooney–Rivlin model is sufficient to characterize the nonlinear behavior of many tissues. Successful applications include animal organs [Bel-Brunon *et al.* (2014)], muscular tissue [Bols *et al.* (2013)], vessels [Karimi *et al.* (2014)], etc. As a linear function of the invariants, it is possible to find analytical solutions for some simple cases. The Mooney–Rivlin model is written as:

$$\Psi_{\text{vol}} = \frac{\kappa}{2}(J-1)^2, \quad (12a)$$

$$\Psi_{\text{iso}} = \frac{\mu_1}{2}(\bar{I}_1 - 3) + \frac{\mu_2}{2}(\bar{I}_2 - 3), \quad (12b)$$

where $\mu_1$, $\mu_2$ and $\kappa$ are material constants. For small deformations, the shear modulus and bulk modulus can be approximated by $\mu_1 + \mu_2$ and $\kappa$. When using mixed formulation Eq. (12a) is rewritten as Eq. (4) where $\Psi_{\text{vol}} = p(J-1)$.

To derive the expression for the PK2 stress, we will first decide $S_{\text{vol}}$ and $S_{\text{iso}}$ separately. The volumetric part of the PK2 stress that is defined in Eq. (8b), can be shown in the following forms:

$$\mathbf{S}_{\text{vol}} = J^{1/3} p \overline{\mathbf{C}}^{-1} \quad (13a)$$

$$J^{1/3}(J-1)\kappa \overline{\mathbf{C}}^{-1}. \quad (13b)$$

Equations (13a) and (13b) are used in the mixed and displacement-based formulations, respectively.

To obtain the isochoric stress $\mathbf{S}_{\text{iso}}$ defined in Eq. (8c), we need to first find the fictitious stress:

$$\begin{aligned} \overline{\mathbf{S}} &= 2\frac{\partial \Psi_{\text{iso}}(\overline{\mathbf{C}})}{\partial \overline{\mathbf{C}}} \\ &= 2\frac{\partial \Psi_{\text{iso}}}{\partial \bar{I}_1}\frac{\partial \bar{I}_1}{\partial \overline{\mathbf{C}}} + 2\frac{\partial \Psi_{\text{iso}}}{\partial \bar{I}_2}\frac{\partial \bar{I}_2}{\partial \overline{\mathbf{C}}} \\ &= \mu_1 \mathbf{I} + \mu_2(\bar{I}_1 \mathbf{I} - \overline{\mathbf{C}}) \\ &= (\mu_1 + \mu_2 \bar{I}_1)\mathbf{I} - \mu_2 \overline{\mathbf{C}}. \end{aligned} \quad (14)$$

With the fourth-order projection tensor $\mathbb{P}$, the isochoric PK2 stress becomes:

$$\begin{aligned} \mathbf{S}_{\text{iso}} &= J^{-2/3}\mathbb{P}:\overline{\mathbf{S}} \\ &= J^{-2/3}\left(\mathbb{I} - \frac{1}{3}\overline{\mathbf{C}}^{-1}\otimes \overline{\mathbf{C}}\right):\overline{\mathbf{S}} \\ &= J^{-2/3}\left[\overline{\mathbf{S}} - \frac{1}{3}(\overline{\mathbf{C}}^{-1}\otimes \overline{\mathbf{C}}):\overline{\mathbf{S}}\right] \\ &= J^{-2/3}\left[\overline{\mathbf{S}} - \frac{1}{3}(\overline{\mathbf{C}}:\overline{\mathbf{S}})\overline{\mathbf{C}}^{-1}\right] \\ &= J^{-2/3}\left\{\overline{\mathbf{S}} - \frac{1}{3}[(\mu_1 + \mu_2\bar{I}_1)\bar{I}_1 - \mu_2(\bar{I}_1{}^2 - 2\bar{I}_2)]\overline{\mathbf{C}}^{-1}\right\} \\ &= J^{-2/3}\left[\overline{\mathbf{S}} - \frac{1}{3}(\mu_1\bar{I}_1 + 2\mu_2\bar{I}_2)\overline{\mathbf{C}}^{-1}\right] \\ &= J^{-2/3}\left[-\frac{1}{3}(\mu_1\bar{I}_1 + 2\mu_2\bar{I}_2)\overline{\mathbf{C}}^{-1} + (\mu_1 + \mu_2\bar{I}_1)\mathbf{I} - \mu_2\overline{\mathbf{C}}\right]. \end{aligned} \quad (15)$$

In the mixed formulation, the volumetric part and isochoric part of the PK2 stress are Eqs. (13a) and (15), respectively since $p$ is independent of $\mathbf{u}$. While in the displacement-based formulation, the two parts are Eqs. (13b) and (15), respectively.

Once the stress is evaluated, the next step is to evaluate the elasticity tensor $\mathbb{C}$ as defined in Eq. (11). Recall that the volumetric elasticity tensor in Eq. (11b) is a function of $\tilde{p}$ where $\tilde{p}$ is

$$\begin{aligned}\widetilde{p} &= p + J\frac{dp}{dJ} \quad (16)\\ &= \kappa(2J-1)\,.\end{aligned}$$

Substituting $\tilde{p}$ into Eq. (11b) and simply evaluating $p$ from Eq. (9), $\mathbb{C}_{\text{vol}}$ becomes

$$\mathbb{C}_{\text{vol}} = J^{-1/3}\widetilde{p}\,\overline{\mathbf{C}}^{-1}\otimes\overline{\mathbf{C}}^{-1} - 2J^{-1/3}p\,\overline{\mathbf{C}}^{-1}\odot\overline{\mathbf{C}}^{-1}, \quad (17a)$$

$$\mathbb{C}_{\text{vol}} = J^{-1/3}(2J-1)\kappa\,\overline{\mathbf{C}}^{-1}\otimes\overline{\mathbf{C}}^{-1} - 2J^{-1/3}(J-1)\kappa\,\overline{\mathbf{C}}^{-1}\odot\overline{\mathbf{C}}^{-1}\,. \quad (17b)$$

Equation (17a) is for the mixed formulation, with $\tilde{p} = p$ because $dp/dJ = 0$, while Eq. (17b) is for the displacement-based formulation.

Next we evaluate $\mathbb{C}_{\text{iso}}$ following Eq. (11c). The first term on the right-hand side in Eq. (11c) requires the evaluation of the fourth-order fictitious elasticity tensor $\mathbb{C}$, which starts with $\partial\Psi_{\text{iso}}/\partial\bar{\mathbf{C}}$:

$$\begin{aligned}\frac{\partial\Psi_{\text{iso}}(\overline{\mathbf{C}})}{\partial\overline{\mathbf{C}}} &= \frac{\mu_1}{2}\frac{\partial\bar{I}_1}{\partial\overline{\mathbf{C}}} + \frac{\mu_2}{2}\frac{\partial\bar{I}_2}{\partial\overline{\mathbf{C}}} \quad (18)\\ &= \frac{\mu_1}{2}\mathbf{I} + \frac{\mu_2}{2}(\bar{I}_1\mathbf{I} - \overline{\mathbf{C}}),\end{aligned}$$

$$\frac{\partial^2\Psi_{\text{iso}}(\overline{\mathbf{C}})}{\partial\overline{\mathbf{C}}\,\partial\overline{\mathbf{C}}} = \frac{\mu_2}{2}\left(\mathbf{I}\otimes\frac{\partial\bar{I}_1}{\partial\overline{\mathbf{C}}} - \mathbb{I}\right) = \frac{\mu_2}{2}(\mathbf{I}\otimes\mathbf{I} - \mathbb{I})\,. \quad (19)$$

Therefore, the fourth-order fictitious elasticity tensor becomes

$$\overline{\mathbb{C}} = 4J^{-4/3}\frac{\partial^2\Psi_{\text{iso}}(\overline{\mathbf{C}})}{\partial\overline{\mathbf{C}}\,\partial\overline{\mathbf{C}}} = 2J^{-4/3}\mu_2(\mathbf{I}\otimes\mathbf{I} - \mathbb{I}), \quad (20)$$

with the projection tensor $\mathbb{P}$, the first term of the right-hand side in Eq. (11c) is:

$$
\begin{aligned}
\mathbb{P}:\overline{\mathbb{C}}:\mathbb{P}^T &= 2J^{-4/3}\mu_2\left(\mathbb{I}-\frac{1}{3}\overline{\mathbf{C}}^{-1}\otimes\overline{\mathbf{C}}\right):(\mathbf{I}\otimes\mathbf{I}-\mathbb{I}):\left(\mathbb{I}-\frac{1}{3}\overline{\mathbf{C}}\otimes\overline{\mathbf{C}}^{-1}\right) \qquad (21)\\
&= 2J^{-4/3}\mu_2\Big[\mathbb{I}:(\mathbf{I}\otimes\mathbf{I}):\mathbb{I}-\frac{1}{3}\mathbb{I}:(\mathbf{I}\otimes\mathbf{I}):(\overline{\mathbf{C}}\otimes\overline{\mathbf{C}}^{-1})-\mathbb{I}:\mathbb{I}:\mathbb{I}\\
&+\mathbb{I}:\mathbb{I}:\frac{1}{3}(\overline{\mathbf{C}}\otimes\overline{\mathbf{C}}^{-1})-\frac{1}{3}(\overline{\mathbf{C}}^{-1}\otimes\overline{\mathbf{C}}):(\mathbf{I}\otimes\mathbf{I}):\mathbb{I}\\
&-\frac{1}{3}(\overline{\mathbf{C}}^{-1}\otimes\overline{\mathbf{C}}):\mathbb{I}:\frac{1}{3}(\overline{\mathbf{C}}\otimes\overline{\mathbf{C}}^{-1})\\
&+\frac{1}{3}(\overline{\mathbf{C}}^{-1}\otimes\overline{\mathbf{C}}):(\mathbf{I}\otimes\mathbf{I}):\frac{1}{3}(\overline{\mathbf{C}}\otimes\overline{\mathbf{C}}^{-1})+\frac{1}{3}(\overline{\mathbf{C}}\otimes\overline{\mathbf{C}}^{-1}):\mathbb{I}:\mathbb{I}\Big]\\
&= 2J^{-4/3}\mu_2\Big[\mathbf{I}\otimes\mathbf{I}-\frac{1}{3}\bar{I}_1(\mathbf{I}\otimes\overline{\mathbf{C}}^{-1})-\mathbb{I}+\frac{1}{3}(\overline{\mathbf{C}}\otimes\overline{\mathbf{C}}^{-1})-\frac{1}{3}\bar{I}_1(\overline{\mathbf{C}}^{-1}\otimes\mathbf{I})\\
&-\frac{1}{9}(\overline{\mathbf{C}}:\overline{\mathbf{C}})(\overline{\mathbf{C}}^{-1}\otimes\overline{\mathbf{C}}^{-1})+\frac{1}{9}\bar{I}_1^2(\overline{\mathbf{C}}^{-1}\otimes\overline{\mathbf{C}})^{-1}+\frac{1}{3}(\overline{\mathbf{C}}^{-1}\otimes\overline{\mathbf{C}})\Big]\\
&= 2J^{-4/3}\mu_2\Big[\mathbf{I}\otimes\mathbf{I}-\mathbb{I}-\frac{1}{3}\bar{I}_1(\overline{\mathbf{C}}^{-1}\otimes\mathbf{I}+\mathbf{I}\otimes\overline{\mathbf{C}}^{-1})\\
&+\frac{1}{3}(\overline{\mathbf{C}}^{-1}\otimes\overline{\mathbf{C}}+\overline{\mathbf{C}}\otimes\overline{\mathbf{C}}^{-1})+\frac{2}{9}\bar{I}_2(\overline{\mathbf{C}}^{-1}\otimes\overline{\mathbf{C}}^{-1})\Big]\\
&= 2J^{-4/3}\mu_2(\mathbf{I}\otimes\mathbf{I}-\mathbb{I})-\frac{2}{3}J^{-4/3}\mu_2\bar{I}_1(\overline{\mathbf{C}}^{-1}\otimes\mathbf{I}+\mathbf{I}\otimes\overline{\mathbf{C}}^{-1})\\
&+\frac{2}{3}J^{-4/3}\mu_2(\overline{\mathbf{C}}^{-1}\otimes\overline{\mathbf{C}}+\overline{\mathbf{C}}\otimes\overline{\mathbf{C}}^{-1})+\frac{4}{9}J^{-4/3}\mu_2\bar{I}_2(\overline{\mathbf{C}}^{-1}\otimes\overline{\mathbf{C}}^{-1}).
\end{aligned}
$$

The second term of the right-hand side of Eq. (11c) requires the trace of $J^{-2/3}\bar{\mathbf{S}}$:

$$
\begin{aligned}
\mathrm{Tr}(J^{-2/3}\overline{\mathbf{S}}) &= J^{-2/3}\overline{\mathbf{S}}:\mathbf{C} \qquad (22)\\
&= \overline{\mathbf{S}}:\overline{\mathbf{C}}\\
&= [(\mu_1+\mu_2\bar{I}_1)\mathbf{I}-\mu_2\overline{\mathbf{C}}]:\overline{\mathbf{C}}\\
&= (\mu_1+\mu_2\bar{I}_1)\bar{I}_1-\mu_2\overline{\mathbf{C}}:\overline{\mathbf{C}}\\
&= (\mu_1+\mu_2\bar{I}_1)\bar{I}_1-\mu_2(\bar{I}_1{}^2-2\bar{I}_2)\\
&= \mu_1\bar{I}_1+2\mu_2\bar{I}_2.
\end{aligned}
$$

Along with the modified projection tensor $\tilde{\mathbb{P}}$, the second term of the right-hand side of Eq. (11c) becomes

$$
\frac{2}{3}\mathrm{Tr}(J^{-2/3}\overline{\mathbf{S}})\tilde{\mathbb{P}} = \frac{2}{3}J^{-4/3}(\mu_1\bar{I}_1+2\mu_2\bar{I}_2)\left(\overline{\mathbf{C}}^{-1}\odot\overline{\mathbf{C}}^{-1}-\frac{1}{3}\overline{\mathbf{C}}^{-1}\otimes\overline{\mathbf{C}}^{-1}\right). \qquad (23)
$$

Finally, with Eq. (15) for $\mathbf{S}_{\mathrm{iso}}$, the third term of the right-hand side of Eq. (11c) becomes

$$
\begin{aligned}
&-\frac{2}{3}(\mathbf{C}^{-1}\otimes\mathbf{S}_{\text{iso}}+\mathbf{S}_{\text{iso}}\otimes\mathbf{C}^{-1}) \qquad (24)\\
&=-\frac{2}{3}J^{-4/3}\left\{\overline{\mathbf{C}}^{-1}\otimes\left[-\frac{1}{3}(\mu_1\bar{I}_1+2\mu_2\bar{I}_2)\overline{\mathbf{C}}^{-1}+(\mu_1+\mu_2\bar{I}_1)\mathbf{I}-\mu_2\overline{\mathbf{C}}\right]\right.\\
&\left.+\left[-\frac{1}{3}(\mu_1\bar{I}_1+2\mu_2\bar{I}_2)\overline{\mathbf{C}}^{-1}+(\mu_1+\mu_2\bar{I}_1)\mathbf{I}-\mu_2\overline{\mathbf{C}}\right]\otimes\overline{\mathbf{C}}^{-1}\right\}\\
&=-\frac{2}{3}J^{-4/3}\left[-\frac{1}{3}(\mu_1\bar{I}_1+2\mu_2\bar{I}_2)(\overline{\mathbf{C}}^{-1}\otimes\overline{\mathbf{C}}^{-1})+(\mu_1+\mu_2\bar{I}_1)(\overline{\mathbf{C}}^{-1}\otimes\mathbf{I})\right.\\
&-\mu_2(\overline{\mathbf{C}}^{-1}\otimes\overline{\mathbf{C}})-\frac{1}{3}(\mu_1\bar{I}_1+2\mu_2\bar{I}_2)(\overline{\mathbf{C}}^{-1}\otimes\overline{\mathbf{C}}^{-1})\\
&\left.+(\mu_1+\mu_2\bar{I}_1)(\mathbf{I}\otimes\overline{\mathbf{C}}^{-1})-\mu_2(\overline{\mathbf{C}}\otimes\overline{\mathbf{C}}^{-1})\right]\\
&=-\frac{2}{3}J^{-4/3}\left[-\frac{2}{3}(\mu_1\bar{I}_1+2\mu_2\bar{I}_2)(\overline{\mathbf{C}}^{-1}\otimes\overline{\mathbf{C}}^{-1})\right.\\
&\left.+(\mu_1+\mu_2\bar{I}_1)(\overline{\mathbf{C}}^{-1}\otimes\mathbf{I}+\mathbf{I}\otimes\overline{\mathbf{C}}^{-1})-\mu_2(\overline{\mathbf{C}}^{-1}\otimes\overline{\mathbf{C}}+\overline{\mathbf{C}}\otimes\overline{\mathbf{C}}^{-1})\right].
\end{aligned}
$$

Combining Eqs. (21), (23) and (24), $\mathbb{C}_{\text{iso}}$ is

$$
\begin{aligned}
&\mathbb{C}_{\text{iso}}=2J^{-4/3}\mu_2(\mathbf{I}\otimes\mathbf{I}-\mathbb{I})-\frac{2}{3}J^{-4/3}\mu_2\bar{I}_1(\overline{\mathbf{C}}^{-1}\otimes\mathbf{I}+\mathbf{I}\otimes\overline{\mathbf{C}}^{-1}) \qquad (25)\\
&+\frac{2}{3}J^{-4/3}\mu_2(\overline{\mathbf{C}}^{-1}\otimes\overline{\mathbf{C}}+\overline{\mathbf{C}}\otimes\overline{\mathbf{C}}^{-1})+\frac{4}{9}J^{-4/3}\mu_2\bar{I}_2(\overline{\mathbf{C}}^{-1}\otimes\overline{\mathbf{C}}^{-1})\\
&+\frac{2}{3}J^{-4/3}(\mu_1\bar{I}_1+2\mu_2\bar{I}_2)\left(\overline{\mathbf{C}}^{-1}\odot\overline{\mathbf{C}}^{-1}-\frac{1}{3}\overline{\mathbf{C}}^{-1}\otimes\overline{\mathbf{C}}^{-1}\right)\\
&+\frac{4}{9}J^{-4/3}(\mu_1\bar{I}_1+2\mu_2\bar{I}_2)(\overline{\mathbf{C}}^{-1}\otimes\overline{\mathbf{C}}^{-1})\\
&-\frac{2}{3}J^{-4/3}(\mu_1+\mu_2\bar{I}_1)(\overline{\mathbf{C}}^{-1}\otimes\mathbf{I}+\mathbf{I}\otimes\overline{\mathbf{C}}^{-1})\\
&+\frac{2}{3}J^{-4/3}\mu_2(\overline{\mathbf{C}}^{-1}\otimes\overline{\mathbf{C}}+\overline{\mathbf{C}}\otimes\overline{\mathbf{C}}^{-1})\\
&=2J^{-4/3}\mu_2(\mathbf{I}\otimes\mathbf{I}-\mathbb{I})+\frac{2}{3}J^{-4/3}(\mu_1\bar{I}_1+2\mu_2\bar{I}_2)\left(\overline{\mathbf{C}}^{-1}\odot\overline{\mathbf{C}}^{-1}-\frac{1}{3}\overline{\mathbf{C}}^{-1}\otimes\overline{\mathbf{C}}^{-1}\right)\\
&-\frac{2}{3}J^{-4/3}(\mu_1+2\mu_2\bar{I}_1)(\overline{\mathbf{C}}^{-1}\otimes\mathbf{I}+\mathbf{I}\otimes\overline{\mathbf{C}}^{-1})\\
&+\frac{4}{3}J^{-4/3}\mu_2(\overline{\mathbf{C}}^{-1}\otimes\overline{\mathbf{C}}+\overline{\mathbf{C}}\otimes\overline{\mathbf{C}}^{-1})+\frac{4}{9}J^{-4/3}(\mu_1\bar{I}_1+3\mu_2\bar{I}_2)\overline{\mathbf{C}}^{-1}\otimes\overline{\mathbf{C}}^{-1}\\
&=2J^{-4/3}\mu_2(\mathbf{I}\otimes\mathbf{I}-\mathbb{I})-\frac{2}{3}J^{-4/3}(\mu_1+2\mu_2\bar{I}_1)(\overline{\mathbf{C}}^{-1}\otimes\mathbf{I}+\mathbf{I}\otimes\overline{\mathbf{C}}^{-1})\\
&+\frac{4}{3}J^{-4/3}\mu_2(\overline{\mathbf{C}}^{-1}\otimes\overline{\mathbf{C}}+\overline{\mathbf{C}}\otimes\overline{\mathbf{C}}^{-1})\\
&+\frac{2}{9}J^{-4/3}(\mu_1\bar{I}_1+4\mu_2\bar{I}_2)(\overline{\mathbf{C}}^{-1}\otimes\overline{\mathbf{C}}^{-1})\\
&+\frac{2}{3}J^{-4/3}(\mu_1\bar{I}_1+2\mu_2\bar{I}_2)(\overline{\mathbf{C}}^{-1}\odot\overline{\mathbf{C}}^{-1}).
\end{aligned}
$$

Equations (17) and (25) complete the derivations of the elasticity tensor for the volumetric and isochoric parts, respectively, in the reference configuration.

**2.3.2. Yeoh model—**First introduced in 1990 [Yeoh (1990)] and modified in 1993 [Yeoh (1993)], Yeoh model was motivated to simulate the mechanical behavior of carbon-black

filled rubber vulcanizates with the typical stiffening effect in large strain domain. Yeoh model is a polynomial of $\bar{I}_1$ only. To capture the stiffening effect of rubber in the large strain domain, it is usually truncated up to the third-order. Yeoh model is another popular choice in biomechanics which has been be applied to human breast tissue [O'Hagen and Samani (2009)], porcine muscular tissue [Bols *et al.* (2013)], rat lung parenchyma [Bel-Brunon *et al.* (2014); Rausch *et al.* (2011)], etc. It is even proven to be the best one in capturing nonlinear behaviors of some specific tissues compared to Neo–Hookean and Mooney–Rivlin models [Zaeimdar (2014)].

The volumetric part to account for compressibility in Yeoh model is the same as in Mooney–Rivlin model. Consequently the volumetric parts of both stress and elasticity tensors are the same as Eqs.(13) and (17). Therefore, we will only show the derivation of the isochoric component.

The isochoric part in Yeoh model includes higher order terms. It is written as:

$$\Psi_{\text{iso}} = c_1(\bar{I}_1 - 3) + c_2(\bar{I}_1 - 3)^2 + c_3(\bar{I}_1 - 3)^3, \quad (26)$$

where $c_1$, $c_2$, $c_3$ are material constants with constraints $c_1 > 0$, $c2 < 0$, and $c_3 > 0$. The initial shear modulus is approximated as $\mu = 2c_1$.

Following the same way, we first derive the fictitious stress:

$$\begin{aligned}\overline{\mathbf{S}} &= 2\frac{\partial \Psi_{\text{iso}}(\overline{\mathbf{C}})}{\partial \overline{\mathbf{C}}} \\ &= 2\frac{\partial \Psi_{\text{iso}}}{\partial \bar{I}_1}\frac{\partial \bar{I}_1}{\partial \overline{\mathbf{C}}} \\ &= [2c_1 + 4c_2(\bar{I}_1 - 3) + 6c_3(\bar{I}_1 - 3)^2]\mathbf{I}.\end{aligned} \quad (27)$$

Then the isochoric part of the PK2 stress is obtained as

$$\begin{aligned}\mathbf{S}_{\text{iso}} &= J^{-2/3}\mathbb{P}:\overline{\mathbf{S}} \\ &= J^{-2/3}\left(\mathbb{I} - \frac{1}{3}\overline{\mathbf{C}}^{-1}\otimes\overline{\mathbf{C}}\right):\overline{\mathbf{S}} \\ &= J^{-2/3}\left[\overline{\mathbf{S}} - \frac{1}{3}(\overline{\mathbf{C}}:\overline{\mathbf{S}})\overline{\mathbf{C}}^{-1}\right] \\ &= J^{-2/3}\left\{\overline{\mathbf{S}} - \frac{1}{3}[2c_1 + 4c_2(\bar{I}_1 - 3) + 6c_3(\bar{I}_1 - 3)^2]\bar{I}_1\overline{\mathbf{C}}^{-1}\right\} \\ &= J^{-2/3}[2c_1 + 4c_2(\bar{I}_1 - 3) + 6c_3(\bar{I}_1 - 3)^2]\left(\mathbf{I} - \frac{1}{3}\bar{I}_1\overline{\mathbf{C}}^{-1}\right).\end{aligned} \quad (28)$$

Similarly, to derive the first term on the right-hand side of Eq. (11c) we must begin with $\partial\Psi_{\text{iso}}/\partial\bar{\mathbf{C}}$:

$$\frac{\partial\Psi_{\text{iso}}(\overline{\mathbf{C}})}{\partial\mathbf{C}} = [c_1 + 2c_2(\bar{I}_1 - 3) + 3c_3(\bar{I}_1 - 3)^2]\frac{\partial\bar{I}_1}{\partial\overline{\mathbf{C}}} \quad (29)$$

$$= [c_1 + 2c_2(\bar{I}_1 - 3) + 3c_3(\bar{I}_1 - 3)^2]\mathbf{I}\,.$$

The second order derivative is

$$\frac{\partial^2\Psi_{\text{iso}}(\overline{\mathbf{C}})}{\partial\overline{\mathbf{C}}\,\partial\overline{\mathbf{C}}} = \mathbf{I}\otimes\frac{\partial[c_1 + 2c_2(\bar{I}_1 - 3) + 3c_3(\bar{I}_1 - 3)^2]}{\partial\overline{\mathbf{C}}} \quad (30)$$

$$= \mathbf{I}\otimes[2c_2\mathbf{I} + 6c_3(\bar{I}_1 - 3)\mathbf{I}]$$

$$= [2c_2 + 6c_3(\bar{I}_1 - 3)]\mathbf{I}\otimes\mathbf{I}\,.$$

Therefore, the fictitious elasticity tensor is

$$\overline{\mathbb{C}} = 4J^{-4/3}\frac{\partial^2\Psi_{\text{iso}}(\overline{\mathbf{C}})}{\partial\overline{\mathbf{C}}\,\partial\overline{\mathbf{C}}} = 8J^{-4/3}[c_2 + 3c_3(\bar{I}_1 - 3)]\mathbf{I}\otimes\mathbf{I}\,. \quad (31)$$

The first term on the right-hand side of Eq. (11c) can be found as

$$\mathbb{P}:\overline{\mathbb{C}}:\mathbb{P}^T = 8J^{-4/3}[c_2 + 3c_3(\bar{I}_1 - 3)]\left(\mathbb{I} - \frac{1}{3}\overline{\mathbf{C}}^{-1}\otimes\overline{\mathbf{C}}\right):(\mathbf{I}\otimes\mathbf{I}):\left(\mathbb{I} - \frac{1}{3}\overline{\mathbf{C}}\otimes\overline{\mathbf{C}}^{-1}\right) \quad (32)$$

$$= 8J^{-4/3}[c_2 + 3c_3(\bar{I}_1 - 3)]\left[\mathbb{I}:(\mathbf{I}\otimes\mathbf{I}):\mathbb{I} - \mathbb{I}:(\mathbf{I}\otimes\mathbf{I}):\frac{1}{3}(\overline{\mathbf{C}}\otimes\overline{\mathbf{C}}^{-1})\right.$$

$$\left. - \frac{1}{3}(\overline{\mathbf{C}}^{-1}\otimes\overline{\mathbf{C}}):(\mathbf{I}\otimes\mathbf{I}):\mathbb{I} + \frac{1}{9}(\overline{\mathbf{C}}^{-1}\otimes\overline{\mathbf{C}}):(\mathbf{I}\otimes\mathbf{I}):(\overline{\mathbf{C}}\otimes\overline{\mathbf{C}}^{-1})\right]$$

$$= 8J^{-4/3}[c_2 + 3c_3(\bar{I}_1 - 3)]$$

$$\times\left[\mathbf{I}\otimes\mathbf{I} - \frac{1}{3}\bar{I}_1(\overline{\mathbf{C}}^{-1}\otimes\mathbf{I}) - \frac{1}{3}\bar{I}_1(\mathbf{I}\otimes\overline{\mathbf{C}}^{-1}) + \frac{1}{9}\bar{I}_1^2(\overline{\mathbf{C}}^{-1}\otimes\overline{\mathbf{C}}^{-1})\right]$$

$$= 8J^{-4/3}[c_2 + 3c_3(\bar{I}_1 - 3)]$$

$$\times\left[\mathbf{I}\otimes\mathbf{I} - \frac{\bar{I}_1}{3}(\mathbf{I}\otimes\overline{\mathbf{C}}^{-1} + \overline{\mathbf{C}}^{-1}\otimes\mathbf{I}) + \frac{\bar{I}_1^2}{9}(\overline{\mathbf{C}}^{-1}\otimes\overline{\mathbf{C}}^{-1})\right]$$

$$= J^{-4/3}[8c_2 + 24c_3(\bar{I}_1 - 3)](\mathbf{I}\otimes\mathbf{I})$$

$$- J^{-4/3}\left[\frac{8}{3}c_2\bar{I}_1 + 8c_3(\bar{I}_1 - 3)\bar{I}_1\right](\mathbf{I}\otimes\overline{\mathbf{C}}^{-1} + \overline{\mathbf{C}}^{-1}\otimes\mathbf{I})$$

$$+ J^{-4/3}\left[\frac{8}{9}c_2\bar{I}_1^2 + \frac{8}{3}c_3(\bar{I}_1 - 3)\bar{I}_1^2\right](\overline{\mathbf{C}}^{-1}\otimes\overline{\mathbf{C}}^{-1}).$$

Using the fictitious PK2 stress derived in Eq. (27), we can obtain the trace of $J^{-2/3}\bar{\mathbf{S}}$:

$$\begin{aligned}\mathrm{Tr}(J^{-2/3}\overline{\mathbf{S}}) &= J^{-2/3}\overline{\mathbf{S}}:\mathbf{C} \\ &= \overline{\mathbf{S}}:\overline{\mathbf{C}} \\ &= [2c_1 + 4c_2(\bar{I}_1 - 3) + 6c_3(\bar{I}_1 - 3)^2](\mathbf{I}:\overline{\mathbf{C}}) \\ &= 2c_1\bar{I}_1 + 4c_2(\bar{I}_1 - 3)\bar{I}_1 + 6c_3(\bar{I}_1 - 3)^2\bar{I}_1.\end{aligned} \quad (33)$$

So that the second term on the right-hand side of Eq. (11c) is

$$\frac{2}{3}\mathrm{Tr}(J^{-2/3}\overline{\mathbf{S}})\widetilde{\mathbb{P}} = \frac{2}{3}J^{-4/3}[2c_1\bar{I}_1 + 4c_2(\bar{I}_1 - 3)\bar{I}_1 + 6c_3(\bar{I}_1 - 3)^2\bar{I}_1] \quad (34)$$
$$\times\left(\overline{\mathbf{C}}^{-1}\odot\overline{\mathbf{C}}^{-1} - \frac{1}{3}\overline{\mathbf{C}}^{-1}\otimes\overline{\mathbf{C}}^{-1}\right)$$
$$= J^{-4/3}\left[\frac{4}{3}c_1\bar{I}_1 + \frac{8}{3}c_2(\bar{I}_1 - 3)\bar{I}_1 + 4c_3(\bar{I}_1 - 3)^2\bar{I}_1\right]\times\left(\overline{\mathbf{C}}^{-1}\odot\overline{\mathbf{C}}^{-1} - \frac{1}{3}\overline{\mathbf{C}}^{-1}\otimes\overline{\mathbf{C}}^{-1}\right).$$

The third term on the right-hand side of Eq. (11c) is obtained by using $\mathbf{S}_{\text{iso}}$ in Eq. 28:

$$
\begin{aligned}
&-\frac{2}{3}J^{-4/3}(\overline{\mathbf{C}}^{-1}\otimes\overline{\mathbf{S}}_{\text{iso}}+\overline{\mathbf{S}}_{\text{iso}}\otimes\overline{\mathbf{C}}^{-1}) \qquad (35)\\
&=-\frac{2}{3}J^{-4/3}[2c_1+4c_2(\bar{I}_1-3)+6c_3(\bar{I}_1-3)^2]\\
&\times\left[\overline{\mathbf{C}}^{-1}\otimes\left(\mathbf{I}-\frac{1}{3}\bar{I}_1\overline{\mathbf{C}}^{-1}\right)+\left(\mathbf{I}-\frac{1}{3}\bar{I}_1\overline{\mathbf{C}}^{-1}\right)\otimes\overline{\mathbf{C}}^{-1}\right]\\
&=J^{-4/3}\left[-\frac{4}{3}c_1-\frac{8}{3}c_2(\bar{I}_1-3)-4c_3(\bar{I}_1-3)^2\right](\overline{\mathbf{C}}^{-1}\otimes\mathbf{I}+\mathbf{I}\otimes\overline{\mathbf{C}}^{-1})\\
&+J^{-4/3}\left[\frac{8}{9}c_1\bar{I}_1+\frac{16}{9}c_2(\bar{I}_1-3)\bar{I}_1+\frac{8}{3}c_3(\bar{I}_1-3)^2\bar{I}_1\right](\overline{\mathbf{C}}^{-1}\otimes\overline{\mathbf{C}}^{-1}).
\end{aligned}
$$

Combining Eqs. (32), (34) and (35), we have the isochoric part of the elasticity tensor:

$$
\begin{aligned}
&\mathbb{C}_{\text{iso}}=J^{-4/3}\left\{[8c_2+24c_3(\bar{I}_1-3)](\mathbf{I}\otimes\mathbf{I}) \qquad (36)\right.\\
&-\left[\frac{4}{3}c_1+c_2\left(\frac{16}{3}\bar{I}_1-8\right)+12c_3(\bar{I}_1-1)(\bar{I}_1-3)\right](\overline{\mathbf{C}}^{-1}\otimes\mathbf{I}+\mathbf{I}\otimes\overline{\mathbf{C}}^{-1})\\
&+\left[\frac{4}{9}c_1\bar{I}_1+c_2\left(\frac{16}{9}\bar{I}_1^2-\frac{8}{3}\bar{I}_1\right)+4c_3\bar{I}_1(\bar{I}_1-1)(\bar{I}_1-3)\right](\overline{\mathbf{C}}^{-1}\otimes\overline{\mathbf{C}}^{-1})\\
&\left.+\left[\frac{4}{3}c_1\bar{I}_1+\frac{8}{3}c_2(\bar{I}_1-3)\bar{I}_1+4c_3(\bar{I}_1-3)^2\bar{I}_1\right](\overline{\mathbf{C}}^{-1}\odot\overline{\mathbf{C}}^{-1})\right\}.
\end{aligned}
$$

Equations (17) and (36) yield the elasticity tensor in the reference configuration for Yeoh model.

**2.3.3. Holzapfel–Gasser–Ogden model—**The Holzapfel–Gasser–Ogden (HGO) model was introduced in 2000 [Holzapfel and Gasser (2000)] to model the layering structure of arterial tissues. The idea was to formulate a constitutive model which incorporates some histological structure of arterial walls (i.e., fiber direction). The volumetric part is the same as Mooney–Rivlin and Yeoh models. What distinguishes HGO model from the phenomenological models is that it accounts for both the non-collagenous matrix material which is active at low pressures (modeled as isotropic) and the collagenous fibers which becomes active at high pressure (modeled as anisotropic). HGO model uses Neo–Hookean model as the isotropic ground material, and the anisotropic part consists two families of fibers represented by two pseudo-invariants $\bar{I}_4$ and $\bar{I}_6$. The directions of these fibers are represented by unit vectors $\mathbf{a}_{04}$ and $\mathbf{a}_{06}$ in the reference configuration. Specifically, the isochoric part of HGO model is consist of isotropic part $\Psi_{\text{isotropic}}$ and anisotropic part $\Psi_{\text{aniso}}$:

$$\Psi_{\text{iso}}(\mathbf{C},\mathbf{a}_{04},\mathbf{a}_{06})=\Psi_{\text{isotropic}}(\overline{\mathbf{C}})+\Psi_{\text{aniso}}(\overline{\mathbf{C}},\mathbf{a}_{04},\mathbf{a}_{06}). \qquad (37a)$$

In particular

$$\Psi_{\text{isotropic}} = \frac{\mu_1}{2}(\bar{I}_1 - 3), \quad (37b)$$

$$\Psi_{\text{aniso}}(\overline{\mathbf{C}}, \mathbf{a}_{04}, \mathbf{a}_{06}) = \frac{k_1}{2k_2} \sum_{i=4,6} \{ \exp [k_2(\bar{I}_i - 1)^2] - 1 \}, \quad (37c)$$

where $k_1 > 0$ is a stress-like material parameter and $k_2 > 0$ is a dimensionless parameter.

The volumetric part of the stress and elasticity tensors of the HGO model are the same as Mooney–Rivlin and Yeoh models derived in Eqs. (13) and (17). The isotropic part of the isochoric HGO model is simply the Neo–Hookean model, which is a special case of Mooney–Rivlin model with $\mu_2 = 0$. Therefore, to obtain the isotropic contribution to the isochoric PK2 stress, we only need to set $\mu_2$ to 0 in Eq. (15)

$$\mathbf{S}_{\text{isotropic}} = J^{-2/3}\mu_1 \left( -\frac{1}{3}\bar{I}_1 \overline{\mathbf{C}}^{-1} + \mathbf{I} \right). \quad (38)$$

Similarly, by setting $\mu_2$ to 0 in the isochoric elasticity tensor from Mooney–Rivlin model in Eq. (25), the isotropic part of the isochoric elasticity tensor for the HGO model becomes:

$$\mathbb{C}_{\text{isotropic}} = -\frac{2}{3}J^{-4/3}\mu_1(\overline{\mathbf{C}}^{-1} \otimes \mathbf{I} + \mathbf{I} \otimes \overline{\mathbf{C}}^{-1}) + \frac{2}{9}J^{-4/3}\mu_1\bar{I}_1\overline{\mathbf{C}}^{-1} \otimes \overline{\mathbf{C}}^{-1} + \frac{2}{3}J^{-4/3}\mu_1\bar{I}_1\overline{\mathbf{C}}^{-1} \odot \overline{\mathbf{C}}^{-1}. \quad (39)$$

To derive the anisotropic parts of stress and elasticity tensors, the deformation of the fibers needs to be introduced. As the material deforms, the vectors of the fibers deform accordingly and are expressed as unit vectors $\mathbf{a}_4$ and $\mathbf{a}_6$ in the current configuration. $\mathbf{a}_{0i}$ and $\mathbf{a}_i$ ($i = 4, 6$) are related by

$$\lambda_i \mathbf{a}_i = \mathbf{F}\mathbf{a}_{0i}, \quad (40)$$

where $i = 4, 6$, $\lambda_i$ is the stretch of the original fiber and no summation is applied on $i$. Since $|\mathbf{a}_i| = 1$, we find the value of stretch $\lambda_i$ through:

$$\lambda_i^2 = \mathbf{a}_{0i} \cdot \mathbf{F}^T \mathbf{F} \mathbf{a}_{0i} = \mathbf{a}_{0i} \cdot \mathbf{C} \mathbf{a}_{0i}, \quad i = 4, 6. \quad (41)$$

To express the anisotropic term, two pseudo-invariants are defined:

$$I_i(\mathbf{C}, \mathbf{a}_{0i}) = \mathbf{a}_{0i} \cdot \mathbf{C} \mathbf{a}_{0i} = \lambda_i^2, \quad i = 4, 6. \quad (42)$$

Similarly, the modified invariants are defined as

$$\bar{I}_i = J^{-2/3} I_i, \quad i = 4, 6. \quad (43)$$

For the convenience of the derivation, we define two second-order tensors to represent the dyadic products of $\mathbf{a}_{0i}$:

$$\mathbf{A}_{0i} = \mathbf{a}_{0i} \otimes \mathbf{a}_{0i}, \quad i = 4, 6. \quad (44)$$

The derivatives of the pseudo-invariants are easy to find

$$\frac{\partial \bar{I}_i}{\partial \overline{\mathbf{C}}} = \mathbf{A}_{0i}, \quad i = 4, 6. \quad (45)$$

Based on the definition of these pseudo-invariants and the symmetric structure of the HGO model itself, it is obvious to see that $\bar{I}_4$ and $\bar{I}_6$ should be symmetric in all the related expressions.

Next, we derive the stress and elasticity tensors for the anisotropic part of the isochoric HGO model in a similar approach as presented in Sec. 2.2. The anisotropic part will be combined with the isochoric isotropic part and the volumetric part to form the complete stress and elasticity tensors of the HGO model.

As the first step, Eq. (45) is used to obtain the anisotropic part of the fictitious PK2 stress:

$$\overline{\mathbf{S}}_{\text{aniso}} = 2 \frac{\partial \Psi_{\text{aniso}}(\overline{\mathbf{C}})}{\partial \overline{\mathbf{C}}} = 2 \sum_{i=4,6} \frac{\partial \Psi_{\text{aniso}}}{\partial \bar{I}_i} \mathbf{A}_{0i}. \quad (46)$$

Recall the definitions in Eqs. (40)–(44), we can prove that

$$\overline{\mathbf{C}}:\mathbf{A}_{0i}=\overline{\mathbf{C}}:(\mathbf{a}_{0i}\otimes\mathbf{a}_{0i})=\mathbf{a}_{0i}\cdot(\overline{\mathbf{C}}\mathbf{a}_{0i})=\bar{I}_i,\quad i=4,6. \tag{47}$$

Consequently,

$$\overline{\mathbf{C}}:\overline{\mathbf{S}}_{\text{aniso}}=2\sum_{i=4,6}\bar{I}_i\frac{\partial\Psi_{\text{aniso}}}{\partial\bar{I}_i}. \tag{48}$$

Using Eq. (48), the isochoric anisotropic PK2 stress is obtained through Eq. (8c)

$$\begin{aligned}\mathbf{S}_{\text{aniso}}&=J^{-2/3}\left(\mathbb{I}-\frac{1}{3}\overline{\mathbf{C}}^{-1}\otimes\overline{\mathbf{C}}\right):\overline{\mathbf{S}}_{\text{aniso}}=J^{-2/3}\left[\overline{\mathbf{S}}_{\text{aniso}}-\frac{1}{3}(\overline{\mathbf{C}}:\overline{\mathbf{S}}_{\text{aniso}})\overline{\mathbf{C}}^{-1}\right] \\ &=2J^{-2/3}\sum_{i=4,6}\left[\frac{\partial\Psi_{\text{aniso}}}{\partial\bar{I}_i}\left(\mathbf{A}_{0i}-\frac{1}{3}\bar{I}_i\overline{\mathbf{C}}^{-1}\right)\right],\end{aligned} \tag{49}$$

where $\partial\Psi_{\text{aniso}}/\partial\bar{I}_i=k_1(\bar{I}_i-1)e^{k_2(\bar{I}_i-1)^2}$. Combining Eqs. (38) and (49), we have the isochoric PK2 stress for the HGO model:

$$\mathbf{S}_{\text{iso}}=J^{-2/3}\mu_1\left(-\frac{1}{3}\bar{I}_1\overline{\mathbf{C}}^{-1}+\mathbf{I}\right)+2J^{-2/3}\sum_{i=4,6}\left[\frac{\partial\Psi_{\text{aniso}}}{\partial\bar{I}_i}\left(\mathbf{A}_{0i}-\frac{1}{3}\bar{I}_i\overline{\mathbf{C}}^{-1}\right)\right]. \tag{50}$$

Next we derive the anisotropic part of the isochoric elasticity tensor of the HGO model. For convenience, we do not explicitly write out $\partial\Psi_{\text{aniso}}/\partial\bar{I}_i$ and $\partial^2\Psi_{\text{aniso}}/\partial\bar{I}_i^2$ where $i=4, 6$. The first and second derivatives of $\Psi_{\text{aniso}}$ with respect to $\bar{\mathbf{C}}$ can be easily converted to that with respect to $\bar{I}_i\,(i=4, 6)$ as follows:

$$\frac{\partial\Psi_{\text{aniso}}}{\partial\overline{\mathbf{C}}}=\sum_{i=4,6}\frac{\partial\Psi_{\text{aniso}}}{\partial\bar{I}_i}\mathbf{A}_{0i}, \tag{51a}$$

$$\frac{\partial^2\Psi_{\text{aniso}}}{\partial\overline{\mathbf{C}}\partial\overline{\mathbf{C}}}=\sum_{i=4,6}\frac{\partial^2\Psi_{\text{aniso}}}{\partial\bar{I}_i^2}\mathbf{A}_{0i}\otimes\mathbf{A}_{0i}. \tag{51b}$$

Using Eq. (51b), the anisotropic contribution to the fictitious elasticity tensor $\bar{\mathbb{C}}_{\text{aniso}}$ is:

$$\overline{\mathbb{C}}_{\text{aniso}} = 4J^{-4/3}\frac{\partial^2\Psi_{\text{aniso}}}{\partial\overline{\mathbf{C}}\partial\overline{\mathbf{C}}} = 4J^{-4/3}\sum_{i=4,6}\frac{\partial^2\Psi_{\text{aniso}}}{\partial\bar{I}_i^2}\mathbf{A}_{0i}\otimes\mathbf{A}_{0i}\,. \quad (52)$$

Therefore, the first term on the right-hand side of Eq. (11c) becomes

$$\begin{aligned}
&\mathbb{P}:\overline{\mathbb{C}}_{\text{aniso}}:\mathbb{P}^T \quad (53)\\
&= \sum_{i=4,6} J^{-4/3}\frac{\partial^2\Psi_{\text{aniso}}}{\partial\bar{I}_i^2}\left(\mathbb{I}-\frac{1}{3}\overline{\mathbf{C}}^{-1}\otimes\overline{\mathbf{C}}\right):(\mathbf{A}_{0i}\otimes\mathbf{A}_{0i}):\left(\mathbb{I}-\frac{1}{3}\overline{\mathbf{C}}\otimes\overline{\mathbf{C}}^{-1}\right)\\
&= \sum_{i=4,6} 4J^{-4/3}\frac{\partial^2\Psi_{\text{aniso}}}{\partial\bar{I}_i^2}\left[\mathbf{A}_{0i}-\frac{1}{3}(\overline{\mathbf{C}}:\mathbf{A}_{0i})\overline{\mathbf{C}}^{-1}\right]\otimes\left[\mathbf{A}_{0i}-\frac{1}{3}(\overline{\mathbf{C}}:\mathbf{A}_{0i})\overline{\mathbf{C}}^{-1}\right]\\
&= \sum_{i=4,6} 4J^{-4/3}\frac{\partial^2\Psi_{\text{aniso}}}{\partial\bar{I}_i^2}\\
&\times\left[\mathbf{A}_{0i}\otimes\mathbf{A}_{0i}-\frac{1}{3}\bar{I}_i(\overline{\mathbf{C}}^{-1}\otimes\mathbf{A}_{0i}+\mathbf{A}_{0i}\otimes\overline{\mathbf{C}}^{-1})+\frac{1}{9}\bar{I}_i^2\overline{\mathbf{C}}^{-1}\otimes\overline{\mathbf{C}}^{-1}\right].
\end{aligned}$$

Recall Eq. (48), the second term on the right-hand side of Eq. (11c) is

$$\begin{aligned}
&\frac{2}{3}\text{Tr}(J^{-2/3}\overline{\mathbf{S}}_{\text{aniso}})\widetilde{\mathbb{P}} = \frac{2}{3}(\overline{\mathbf{S}}_{\text{aniso}}:\overline{\mathbf{C}})\widetilde{\mathbb{P}} \quad (54)\\
&= \frac{2}{3}J^{-4/3}(\overline{\mathbf{S}}_{\text{aniso}}:\overline{\mathbf{C}})\left(\overline{\mathbf{C}}^{-1}\odot\overline{\mathbf{C}}^{-1}-\frac{1}{3}\overline{\mathbf{C}}^{-1}\otimes\overline{\mathbf{C}}^{-1}\right)\\
&= \sum_{i=4,6}\frac{4}{3}J^{-4/3}\bar{I}_i\frac{\partial\Psi_{\text{aniso}}}{\partial\bar{I}_i}\left(\overline{\mathbf{C}}^{-1}\odot\overline{\mathbf{C}}^{-1}-\frac{1}{3}\overline{\mathbf{C}}^{-1}\otimes\overline{\mathbf{C}}^{-1}\right).
\end{aligned}$$

Substituting Eq. (49) into the third term on the right-hand side of Eq. (11c), it becomes:

$$\begin{aligned}
&-\frac{2}{3}J^{-2/3}(\overline{\mathbf{C}}^{-1}\otimes\mathbf{S}_{\text{aniso}}+\mathbf{S}_{\text{aniso}}\otimes\overline{\mathbf{C}}^{-1}) \quad (55)\\
&= \sum_{i=4,6}-\frac{4}{3}J^{-4/3}\frac{\partial\Psi_{\text{aniso}}}{\partial\bar{I}_i}\\
&\times\left[\overline{\mathbf{C}}^{-1}\otimes\left(\mathbf{A}_{0i}-\frac{1}{3}\bar{I}_i\overline{\mathbf{C}}^{-1}\right)+\left(\mathbf{A}_{0i}-\frac{1}{3}\bar{I}_i\overline{\mathbf{C}}^{-1}\right)\otimes\overline{\mathbf{C}}^{-1}\right]\\
&= \sum_{i=4,6}-\frac{4}{3}J^{-4/3}\frac{\partial\Psi_{\text{aniso}}}{\partial\bar{I}_i}\left(\overline{\mathbf{C}}^{-1}\otimes\mathbf{A}_{0i}+\mathbf{A}_{0i}\otimes\overline{\mathbf{C}}^{-1}-\frac{2}{3}\bar{I}_i\overline{\mathbf{C}}^{-1}\otimes\overline{\mathbf{C}}^{-1}\right).
\end{aligned}$$

Adding up Eqs. (53)–(55), we have the anisotropic part of the isochoric elasticity tensor for the HGO model:

$$\mathbb{C}_{\text{aniso}} = \sum_{i=4,6} J^{-4/3}\left[4\frac{\partial^2\Psi_{\text{aniso}}}{\partial\bar{I}_i^2}(\mathbf{A}_{0i}\otimes\mathbf{A}_{0i}) - \frac{4}{3}\left(\bar{I}_i\frac{\partial^2\Psi_{\text{aniso}}}{\partial\bar{I}_i^2}+\frac{\partial\Psi_{\text{aniso}}}{\partial\bar{I}_i}\right)(\overline{\mathbf{C}}^{-1}\otimes\mathbf{A}_{0i}+\mathbf{A}_{0i}\otimes\overline{\mathbf{C}}^{-1}) + \frac{4}{9}\left(\bar{I}_i^2\frac{\partial^2\Psi_{\text{aniso}}}{\partial\bar{I}_i^2}+\bar{I}_i\frac{\partial\Psi_{\text{aniso}}}{\partial\bar{I}_i}\right)(\overline{\mathbf{C}}^{-1}\otimes\overline{\mathbf{C}}^{-1}) + \frac{4}{3}\bar{I}_i\frac{\partial\Psi_{\text{aniso}}}{\partial\bar{I}_i}(\overline{\mathbf{C}}^{-1}\odot\overline{\mathbf{C}}^{-1})\right], \tag{56}$$

where the $\partial\Psi_{\text{aniso}}/\partial\bar{I}_i$ and $\partial^2\Psi_{\text{aniso}}/\partial\bar{I}_i^2$ ($i = 4, 6$) are given in Eq. (51).

Combining Eq. (39) with Eq. (56), the complete isochoric part of the elasticity tensor of HGO model is

$$\mathbb{C}_{\text{iso}} = -\frac{2}{3}J^{-4/3}\mu_1(\overline{\mathbf{C}}^{-1}\otimes\mathbf{I}+\mathbf{I}\otimes\overline{\mathbf{C}}^{-1}) + \frac{2}{9}J^{-4/3}\mu_1\bar{I}_1(\overline{\mathbf{C}}^{-1}\otimes\overline{\mathbf{C}}^{-1}) + \frac{2}{3}J^{-4/3}\mu_1\bar{I}_1(\overline{\mathbf{C}}^{-1}\odot\overline{\mathbf{C}}^{-1}) + \sum_{i=4,6} J^{-4/3}\left[4\frac{\partial^2\Psi_{\text{aniso}}}{\partial\bar{I}_i^2}(\mathbf{A}_{0i}\otimes\mathbf{A}_{0i}) - \frac{4}{3}\left(\bar{I}_i\frac{\partial^2\Psi_{\text{aniso}}}{\partial\bar{I}_i^2}+\frac{\partial\Psi_{\text{aniso}}}{\partial\bar{I}_i}\right)(\overline{\mathbf{C}}^{-1}\otimes\mathbf{A}_{0i}+\mathbf{A}_{0i}\otimes\overline{\mathbf{C}}^{-1}) + \frac{4}{9}\left(\bar{I}_i^2\frac{\partial^2\Psi_{\text{aniso}}}{\partial\bar{I}_i^2}-\bar{I}_i\frac{\partial\Psi_{\text{aniso}}}{\partial\bar{I}_i}\right)(\overline{\mathbf{C}}^{-1}\otimes\overline{\mathbf{C}}^{-1}) + \frac{4}{3}\bar{I}_i\frac{\partial\Psi_{\text{aniso}}}{\partial\bar{I}_i}(\overline{\mathbf{C}}^{-1}\odot\overline{\mathbf{C}}^{-1})\right]. \tag{57}$$

The volumetric part of the elasticity tensor is still the same as Eq. (17).

Table 1 lists a summary of the derived tensors in the reference configuration for all three models, namely Mooney–Rivlin, Yeoh and HGO. An updated Lagrangian formulation can be derived by using a push-forward approach based on the reference configuration. The detailed derivation can be found in Appendix A. The corresponding summary of equations in the current configuration is shown in Table 2.

## 3. Numerical Experiments

In this section, we present two sets of test cases to validate the derived formulas. The first case is a biaxial tension test which is often used to calibrate material constants. For isotropic materials, the analytical solution can be easily found if the material is assumed to be incompressible. The Poisson's ratio for all the test cases is set to $\nu = 0.49999$, which is nearly incompressible where the volume is checked to be unchanged with double machine

precision. For extreme cases, such as an even high Poisson's ratio or absolutely incompressible material (which is hardly meaningful in reality) where $\nu = 0.5$, using the typical displacement-based formulation would result in numerical problems such as locking. We must then resolve it with mixed formulation. The second case is the expansion of a 2D cylinder. It is widely used to validate numerical simulations as the theoretical solutions can often be found for simple models. The results of both cases are obtained in updated Lagrangian formulation, using the formulas listed in Table 2.

### 3.1. Biaxial tension test

In this test, we examine the three isotropic models (Neo–Hookean, Mooney–Rivlin, and Yeoh models) and 1 anisotropic HGO model. Consider a long bar loaded equally in two directions with fixed tractions. The section of the bar is a 1 $m^2$-square. As shown in Fig. 1, the back surface is fixed in the $x$ direction; the left surface is fixed in the $y$ direction and the bottom surface is fixed in the $z$ direction. External tractions are applied to the front and right surfaces.

The bar is stretched by the tractions in $x$ and $y$ directions, and compressed in the $z$ direction in order to maintain the volume. The stretch $\lambda$ is defined as the ratio between the deformed length to the original length in $x$ and $y$ directions. For an isotropic incompressible material, the deformation tensor can be written as

$$\mathbf{F} = \begin{bmatrix} \lambda & 0 & 0 \\ 0 & \lambda & 0 \\ 0 & 0 & \lambda^{-2} \end{bmatrix}. \quad (58)$$

Based on Eq. (58) the theoretical solution of the diagonal components of the PK2 stress is expressed as:

$$S_{11} = S_{22} = 2(1 - \lambda^{-6})\left(\frac{\partial \Psi_{\text{iso}}}{\partial \bar{I}_1} + \lambda^2 \frac{\partial \Psi_{\text{iso}}}{\partial \bar{I}_2}\right) \quad (59)$$

$$S_{33} = 0.$$

All the off-diagonal components are 0. Note that the theoretical solution is not limited in the range of small deformation since no such assumption is made.

Since the nonzero components of the PK2 stress are the same, we denote them as $S$. For Mooney–Rivlin model, plug Eq. (12b) into (59), we have

$$S = (1 - \lambda^{-6})(\mu_1 + \mu_2 \lambda^2). \quad (60)$$

Therefore, the nominal stress $P$ is

$$P = \lambda S = (\lambda - \lambda^{-5})(\mu_1 + \mu_2\lambda^2). \quad (61)$$

When $\mu_2 = 0$ terms we have the nominal stress for Neo–Hookean model:

$$P = \lambda S = \mu_1(\lambda - \lambda^{-5}). \quad (62)$$

Similarly, for Yeoh model:

$$P = \lambda S = 2(\lambda - \lambda^{-5}) \times [c_1 + 2c_2(2\lambda^2 + \lambda^{-4} - 3) + 3c_3(2\lambda^2 + \lambda^{-4} - 3)^2]. \quad (63)$$

Table 3 lists the material constants used in the isotropic models, which are curve-fitted from the standard ASTM412 tensile test results of the rubber used in the transmission mounts [Sharma (2003)].

Figure 2(a) shows the results of the theoretical calculations and numerical computations for all three isotropic models for $\lambda$ in the range of 1 to 1.8. Since the traction is fixed in the original configuration, the nominal stress equals the traction. Perfect agreement is achieved at every discrete data point. As expected, in the small strain range, all these models have similar linear performance. It can be seen that $\mu_2$ in Mooney–Rivlin model acts as a modification to $\mu_1$ in Neo–Hookean model which increases the stiffness. In large strain range, the stiffness of Yeoh model grows quickly, becoming significantly larger than the others due to the inclusion of the higher order terms.

To demonstrate the anisotropy of HGO model, we compare the stretches in two directions in the biaxial tension test. We use the material parameters calibrated from the media layer of the artery in Holzapfel and Gasser [2000] but only one direction is strengthened. That is, both two families of fibers are arranged in the same direction while the tractions are still applied in two directions. The material parameters are $\mu_1 = 3$KPa, $k_1 = 2.3632$KPa, $k_2 = 0.8393$ and $\kappa = 1\times10^5$ KPa. We vary the direction of the fibers measured by the angle from the $x$ direction denoted as $\alpha$, from 0° to 90° to observe the trends qualitatively as there is no existing theoretical solution.

The stretch ratio $\lambda$ is defined as $\lambda = \begin{cases} \lambda_y/\lambda_x, & \alpha = 0°, 30° \text{ or } 45° \\ \lambda_x/\lambda_y, & \alpha = 60° \text{ or } 90° \end{cases}$, where $\lambda_y$ is greater than $\lambda_x$ when $0° < \alpha < 45°$ since the $x$ direction is strengthened more. As the angle gets larger, $\lambda_x$ becomes greater too. Figure 2(b) shows the nominal stress, which is nothing but the traction applied to each surface, as a function of the stretch ratio. As expected, the stretch ratio at $\alpha = 0°$ is the same as $\alpha = 90°$. These complementary angles of $\alpha$ yields the most asymmetric results since the stretch ratio is the largest for a given nominal stress. Same stretch ratios are

obtained for $\alpha = 30°$ and $\alpha = 60°$. When $\alpha = 45°$ two directions become symmetric and the stretch ratio remains to be 1.

### 3.2. Cylindrical pressure vessel with isotropic models

In the second test, we consider a vessel under internal pressure. This case is more challenging than the previous one, especially in the Cartesian coordinates system since the deformation varies both in the radial and the circumferential directions. As shown in Fig. 3, the cylinder has an internal radius of $R_i = 7$m and an external radius of $R_o = 18.625$ m. Only a quarter of vessel is considered with plain strain assumption. Symmetry conditions are applied to the two sides to simulate a complete cylinder. The material parameters for the isotropic models are the same as the previous example, listed in Table 3.

As a benchmark, we model the vessel with Mooney–Rivlin model and compare the radial displacement, hoop stress, radial stress, and axial stress with the analytical solutions. For incompressible materials, the analytical solutions are found in Green and Zerna [1968] as follows:

$$u_r = -R + \sqrt{R^2 + b}, \quad (64a)$$

Fig. 3. Cross-section of the vessel.

$$\sigma_{\theta\theta} = p + \mu_2 + (\mu_1 + \mu_2)\left(\frac{r}{R}\right)^2 + C, \quad (64b)$$

$$\sigma_{rr} = p + \mu_2 + (\mu_1 + \mu_2)\left(\frac{R}{r}\right)^2 + C, \quad (64c)$$

$$\sigma_{zz} = p + \mu_1 + \mu_2\left[\left(\frac{R}{r}\right)^2 + \left(\frac{r}{R}\right)^2\right] + C, \quad (64d)$$

$$p = -p_i - \mu_2 - (\mu_1 + \mu_2) \times \left(\log\frac{r}{R_i} + \frac{b}{2}(r^2 - R_i^2) - \log\frac{R}{R_i} + \left(\frac{R_i}{r}\right)^2\right), \quad (64e)$$

where $R$ and $r$ are the radial coordinate before and after deformation, $p$ is the hydrostatic pressure, $u_r$ is the radial displacement, and $\sigma_{\theta\theta}$, $\sigma_{rr}$ and $\sigma_{zz}$ are the hoop, radial and axial stresses, respectively. $C$ is an arbitrary constant to be determined by the reference pressure since the material is incompressible. $b$ is a constant determined by the internal pressure $p_i$ as

$$p_i = 2(\mu_1 + \mu_2) \times \left( \log \frac{R_i^2 + b}{R_o^2 + b} - 2 \log \frac{R_i}{R_o} + b \frac{R_o^2 - R_i^2}{(R_o^2 + b)(R_i^2 + b)} \right). \quad (64f)$$

Again, this solution is not limited in the range of small deformation.

Figure 4 shows the stress components and the radial displacement along the radial direction under a given internal pressure of $p_i$ = 200KPa. Good agreement is achieved on all the components. There are 21 nodes that are uniformly distributed in the radial direction. As expected, point on the outer surface undergoes less radial displacement than the inner surface in order to keep the area of cross-section unchanged. All the components of the Cauchy stress exhibit nonuniform distribution. The absolute value of hoop stress and radial stress on the inner surface are more significant than the outer surface. This is not altered by the value of the material constants or the pressure. But by setting different material constants along the radial direction one can obtain more uniform stress distributions Batra (1980). Note that the axial stress is usually challenging to validate as they are seldomly shown in literature. The responses of a range of internal pressures are also studied. We pick the node at the midpoint in the radial direction ($R$ = 12.8125m) and study its deformation under different internal pressures from 50KPa to 350KPa. As shown in Fig. 5, the computational result and analytical solution agree perfectly with each other. The variation of the radial displacement and the stress are nonlinear in the sense that the absolute value increases faster at greater pressure. This is similar to what we observed in Fig. 2(a).

With the validated implementation of the Mooney–Rivlin model, we then compare the performance of Neo–Hookean, Mooney–Rivlin, and Yeoh model. Figure 6 shows the results of these models under an inner pressure of $p_i$ = 350KPa. All these isotropic models have similar trends, and the discrepancies among different models decrease from the inner surface to the outer surface. It implies that under a moderate pressure, different isotropic models do not make too much difference. The performance of the Yeoh model is very close to the Neo–Hookean model and stiffening effect does not occur. This is because they both have only one invariant and the strain is not large enough for Yeoh model to demonstrate its particular characteristics due to the higher order term. Considering in this case the maximum strain is already significant, and the expansion of vessels is not likely to exceed this maximum, it is expected that Yeoh model and Neo–Hookean model behave similarly.

## 4. Concluding Remarks

In order to implement any model with finite element method efficiently, one has to find a general way to derive the stress and elasticity tensors. In this paper, we presented a systematic way to do that by decomposing the strain–energy function, stress tensor, and the elasticity tensor into volumetric and isochoric parts. We derived the stress and elasticity tensors for the Mooney–Rivlin, Yeoh, and HGO model as examples. These models are popular in biomechanics and cover both isotropic and anisotropic models. Incompressibility in biomaterials was also discussed, where the tangent stiffness matrix of the standard displacement-based formulation is often ill-conditioned. Toward this end, the volumetric

parts of the derived formulas are rewritten as functions of the pressure so that mixed formulation can be implemented. Two numerical experiments were examined that include biaxial tension, and vessel expansion. These experiments involved Neo–Hookean, Mooney–Rivlin, Yeoh and HGO models. Their comparisons to analytical solutions and existing numerical solutions yielded excellent agreement. In summary, this paper addressed the challenges in the derivation of the stress and elasticity tensors for hyperelastic models using the existing literature by providing a framework with detailed procedure. It will be useful to the researchers in computational biomechanics. Following the systematic approach, readers should be able to derive stress and elasticity tensors for any hyperelastic model as part of their own code or as user-define functions in finite element packages.

## References


Abaqus. Abaqus Theory Manual. Dassault Systemes Simulia Corporation; 2014.

Baaijens FPT. 1998; Mixed finite element methods for viscoelastic flow analysis: A review. J Non-Newtonian Fluid Mech. 79:361–385.

Bathe, KJ. Finite Element Procedures. Klaus-Jurgen Bathe; 2014.

Batra RC. 1980; Finite plane strain deformations of rubberlike materials. Int J Numer Methods Eng. 15:145–160.

Bel-Brunon A, Kehl S, Martin C, Uhlig S, Wall WA. 2014; Numerical identification method for the non-linear viscoelastic compressible behavior of soft tissue using uniaxial tensile tests and image registration — Application to rat lung parenchyma. J Mech Behav Biomech Mater. 29:360–374.

Belytschko, T, Liu, WK, Moran, B. Nonlinear Finite Elements for Continua and Structures. Wiley; 2000.

Bols J, Degroote J, Trachet B, Verhegghe B, Segers P, Vierendeels J. 2013; A comparative study of several material models for prediction of hyperelastic properties: Application to silicone-rubber and soft tissues. J Comput Appl Math. 246:10–17.

Bols J, Degroote J, Trachet B, Verhegghe B, Segers P, Vierendeels J. 2013; Finite element modelling of cell wall properties for onion epidermis using a fibre-reinforced hyperelastic model. J Comput Appl Math. 246:10–17.

de Borst R. 1988; Modelling and analysis of rubberlike materials. Heron. 33:1–56.

Bower, AF. Applied Mechanics of Solids. CRC Press; 2009.

COMSOL. COMSOL Multiphysics User’s Guide. COMSOL Inc; 2012.

Cervera M, Chiumenti M, Codina R. 2010; Mixed stabilized finite element methods in nonlinear solid mechanics Part I: Formulation. Comput Methods Appl Mech Eng. 199:2559–2570.

Chuong CJ, Fung YC. 1983; Three-dimensional stress distribution in arteries. J Biomech Eng. 105:268–274. [PubMed: 6632830]

Chuong CJ, Fung YC. 1986; On residual stress in arteries. J Biomech Eng. 108:189–192. [PubMed: 3079517]

Demiray H. 1972; A note of elasticity of soft biological tissues. J Biomech. 5:309–311. [PubMed: 4666535]

Fu YB, Chui CK, Teo CL. 2013; Liver tissue characterization from uniaxial stress–strain data using probabilistic and inverse finite element methods. J Mech Behav Biomech Mater. 20:105–112.

Fung YC. 1967; Elasticity of soft tissues in simple elongation. Am J Physiol. 213:1532–1544. [PubMed: 6075755]

Fung, YC. Biomechanics: Mechanical Properties of Living Tissues. Springer-Verlag; New York: 1993.

Gajewski M, Szczerba R, Jemiolo S. 2015; Modelling of elastomeric bearings with application of Yeoh hyperelastic material model. Proc Eng. 111:220–227.

Green, AE, Zerna, W. Theoretical Elasticity. Oxford University Press; 1968.

Guo X, Liu Y, Kassab GS. 2012; Diameter-dependent axial prestretch of porcine coronary arteries and veins. J Appl Physiol. 112:982–989. [PubMed: 22162531]

Herrmann LR. 1965; Elasticity equations for incompressible and nearly incompressible materials by a variational theorem. AIAA J. 3:1896–1900.

Holzapfel, GA. Nonlinear Solid Mechanics: A Continuum Approach for Engineering. Wiley; 2000.

Holzapfel GA, Gasser TC. 2000; A new constitutive framework for arterial wall mechanics and a comparative study of material models. J Elasticity. 61:1–48.

Holzapfel, GA, Ogden, RW. Biomechanics of Soft Tissue in Cardiovascular Systems. Springer-Verlag; Wien: 2003.

Hu H. 1954; On some variational principles in the theory of elasticity and the theory of plasticity. Acta Phys Sin. 10:259–290.

Karimi A, Navidbakhsh M, Alizadeh M, Shojaei A. 2014; A comparative study on the mechanical properties of the umbilical vein and umbilical artery under uniaxial loading. Artery Res. 8:51–56.

Karimi A, Navidbakhsh M, Beigzadeh B, Faghihi S. 2013; Hyperelastic mechanical behavior of rat brain infected by Plasmodium berghei ANKA — experimental testing and constitutive modelling. Int J Damage Mech. 0:1–15.

Kaster T, Sack I, Samani A. 2011; Measurement of the hyperelastic properties of ex vivo brain tissue slices. J Biomech. 44:1158–1163. [PubMed: 21329927]

Li Y, Tang S, Kroger M, Liu WK. 2016; Molecular simulation guided constitutive modeling on finite strain viscoelasticity of elastomers. J Mech Phys Solids. 88:204–226.

Maltzahn WW, Von Warriyar RG, Keitzer WF. 1984; Experimental measurments of elastic properties of media and adventitia of bovine carotid arteries. J Biomech. 17:839–847. [PubMed: 6520132]

Mass SA, Ellis BJ, Ateshian GA, Weiss JA. 2012; FEBio: Finite elements for biomechanics. J Biomech Eng. 134:1–10.

Masson I, Boutouyrie P, Laurent S, Humphrey JD, Zidi M. 2008; Characterization of arterial wall mechanical behavior and stresses from human clinical data. J Biomech. 41:2618–2627. [PubMed: 18684458]

Masson I, Fassot C, Zidi M. 2010; Finite dynamic deformations of a hyperelastic, anisotropic, incompressible and prestressed tube. Applications to in vivo arteries. Eur J Mech A/Solids. 29:523–529.

Mooney M. 1940; A theory of large elastic deformation. J Appl Phys. 11:582–592.

Nicholson DW. 1995; Tangent modulus matrix for finite element analysis of hyperelastic materials. Acta Mech. 112:187–201.

Oberai AA, Gokhale NH, Goenezen S, Barbone PE, Hall TJ, Sommer AM, Jiang J. 2009; Linear and nonlinear elasticity imaging of soft tissue in vivo: Demonstration of feasibility. Phys Med Biol. 54:1191–1207. [PubMed: 19182325]

Oden, JT. Finite Elements of Nonlinear Continua. Dover Publications; 2006.

Ogden RW. 1972; Large deformation isotropic elasticity-on the correlation of theory and experiment for incompressible rubberlike solids. Proc R Soc Lond A Math Phys Eng Sci. 326:565–584.

O'Hagen JJ, Samani A. 2009; Measurement of the hyperelastic properties of 44 pathological ex vivo breast tissue samples. Phys Med Biol. 54:2557–2569. [PubMed: 19349660]

Ohayon J, Dubreuil O, Tracqui P, Floc'h S, Le Rioufol G, Chalabreysse L, Thivolet F, Pettigrew RI, Finet G. 2007Influence of residual stress/strain on the biomechanical stability of vulnerable coronary plaques: Potential impact for evaluating the risk of plaque rupture. Am J Physiol Heart Circulatory Physiol. 293:H1987–H1996.

Papadopoulos P, Taylor RL. 1992; A mixed formulation for the finite elment solution of contact problems. Comput Methods Appl Mech Eng. 94:373–389.

Qian M, Wells DM, Jones A, Becker A. 2010; Finite element modelling of cell wall properties for onion epidermis using a fiber-reinforced hyperelastic model. J Struct Biol. 172:300–304. [PubMed: 20800094]

Rashid B, Destrade M, Gilchrist MD. 2013; Mechanical characterization of brain tissue in simple shear at dynamic strain rates. J Mech Behav Biomech Mater. 28:71–85.

Rausch SMK, Martin C, Bornemann PB, Uhlig S, Wall WA. 2011; Material model of lung parenchyma based on living precision — cut lung slice testing. J Mech Behav Biomech Mater. 4:583–592.

Rhodin, JAG. Handbook of Physiology, The Cardiovascular System. John Wiley and Sons; 1980.

Rivlin RS. 1948; Large elastic deformations of isotropic materials. Philos Trans R Soc Lond A Math Phys Eng Sci. 241:379–397.

Saraf H, Ramesh KT, Lennon AM, Merkle AC, Roberts JC. 2007; Mechanical properties of soft human tissues under dynamic loading. J Biomech. 40:1960–1967. [PubMed: 17125775]

Sharma, S. Critical Comparison of Popular Hyper-Elastic Material Models in Design of Anti-Vibration Mounts for Automotive Industry Through FEA. Swets and Zeitlinger; 2003.

Simo JC, Rifai MS. 1990; A class of mixed assumed strain methods and the method of incompatible modes. Int J Numer Methods Eng. 29:1595–1638.

Steinmann P, Hossain M, Possart G. 2012; Hyperelastic models for rubber-like materials: Consistent tangent operators and suitability for Treloar's data. Arch Appl Mech. 82:1183–1217.

Suchocki C. 2011; A finite element implementation of Knowles stroed-energy function: Theory, coding and applications. Arch Mech Eng. LVIII:319–346.

Umale S, Deck C, Bourdet N, Dhumane P, Soler L, Marescaux J, Winger R. 2013; Experimental mechanical characterization of abdominal organs: Liver, kidney and spleen. J Mech Behav Biomech Mater. 17:22–33.

Untaroiu CD, Lu YC, Siripurapu SK, Kemper AR. 2015; Modeling the biomechanics and injury response of human liver parenchyma under tensile loading. J Mech Behav Biomech Mater. 41:280–291.

Veronda DR, Westmann RA. 1970; Mechanical characterization of skin-finite deformations. J Biomech. 3:111–124. [PubMed: 5521524]

de Veubeke, BF. Displacement and Equilibrium Models in the Finite Element Method. Wiley; 1965.

Weiss JA, Maker BN, Govindjee S. 1996; Finite element implementation of incompressible, transversely isotropic hyperelasticity. Comput Methods Appl Mech Eng. 135:107–128.

Wex C, Arndt S, Stoll A, Bruns C, Kupriyanova Y. 2015; Isotropic incompressible hyperelastic models for modelling the mechanical behaviour of biological tissues: A review. Biomed Tech (Berl). 60:577–592. [PubMed: 26087063]

Xie J, Zhou J, Fung YC. 1995; Bending of blood vessel wall: Stress-strain laws of the intima-media and adventitial layers. J Biomech Eng. 117:136–145. [PubMed: 7609477]

Yeoh OH. 1993; Some forms of the strain energy function for rubber. Rubber Chem Technol. 66:754–771.

Yeoh OH. 1990; Characterization of elastic properties of carbon black filled rubber vulcanizates. Rubber Chem Technol. 63:792–805.

Zaeimdar, S. Mechanical Characterization of Breast Tissue Constituents for Cancer Assessment. Simon Fraser University; 2014.

Zhao J, Liao D, Chen P, Kunwald P, Gregersen H. 2008; Stomach stress and strain depend on location, direction and the layered structure. J Biomech. 41:3441–3447. [PubMed: 19004444]

Zienkiewicz, OC, Taylor, RL. The Finite Element Method for Solid and Structural Mechanics. Elsevier; 2005.

## Appendix A. Updated Lagrangian Formulation

In the updated Lagrangian Formulation, the Kirchhoff stress $\boldsymbol{\tau}$ or the Cauchy stress $\boldsymbol{\sigma}$ is used instead of the PK2 stress **S**, meanwhile the principle of virtual work or principle of stationary potential energy and their linearization are written in the current configuration as well. In this appendix we will show the corresponding formulations in the current configuration.

The stress tensor we work with in the updated Lagrangian formulation is the Kirchhoff stress $\boldsymbol{\tau}$, which is obtained by a push-forward operation of the PK2 stress **S**:

$$\boldsymbol{\tau} = \mathbf{F}\mathbf{S}\mathbf{F}^T. \quad \text{(A.1)}$$

Recall the definition of the elasticity tensor $\mathbb{C}$ in Eq. (10), the spatial tensor of elasticity $\mathbb{C}$ is defined as

$$\mathbb{C} = \frac{\partial \mathscr{L}_{\mathbf{v}}(\boldsymbol{\tau}^{\sharp})}{\partial \mathbf{d}}, \quad \text{(A.2)}$$

where $\mathscr{L}_{\mathbf{v}}(\boldsymbol{\tau}^{\sharp})$ is the objective Oldroyd stress rate defined as: $\mathscr{L}_{\mathbf{v}}(\boldsymbol{\tau}^{\sharp}) = \dot{\boldsymbol{\tau}} - \mathbf{l}\boldsymbol{\tau} - \boldsymbol{\tau}\mathbf{l}^T$, $\mathbf{l} = \nabla_{\mathbf{x}}\mathbf{v}$ and $\mathbf{d} = (\mathbf{l} + \mathbf{l}^T)/2$. The spatial tensor of elasticity $\mathbb{C}$ can be transformed from the elasticity tensor $\mathbb{C}$ through a push-forward operation

$$c_{ijkl} = F_{iI}F_{jJ}F_{kK}F_{lL}C_{IJKL}. \quad \text{(A.3)}$$

Next we will derive the Kirchhoff stress $\boldsymbol{\tau}$ and the spatial tensor of elasticity $\mathbb{C}$ for Mooney–Rivlin model, Yeoh model and HGO model respectively. All these models have the same volumetric part, which can be obtained by substituting Eq. (13) into Eq. (A.1):

$$\boldsymbol{\tau}_{\text{vol}} = \mathbf{F}\mathbf{S}_{\text{vol}}\mathbf{F}^T, \quad \text{(A.4a)}$$

$$= Jp\mathbf{I}, \quad \text{(A.4b)}$$

$$= J(J-1)\kappa\mathbf{I}. \quad \text{(A.4c)}$$

Substituting Eq. (17) into Eq. (A.3) gives the volumetric spatial tensor of elasticity. For convenience, here we use the index notation:

$$(c_{\text{vol}})_{ijkl} = F_{iI}F_{jJ}F_{kK}F_{lL}(C_{\text{vol}})_{IJKL} \quad \text{(A.5a)}$$

$$= J\tilde{p}\delta_{ij}\delta_{kl} - Jp(\delta_{ik}\delta_{jl} + \delta_{il}\delta_{jk}) \quad \text{(A.5b)}$$

$$= \kappa[J(2J-1)\delta_{ij}\delta_{kl} - J(J-1)(\delta_{ik}\delta_{jl} + \delta_{il}\delta_{jk})]\,. \quad \text{(A.5c)}$$

Equations (A.4) and (A.5) complete the volumetric part of the Kirchhoff stress and spatial tensor of elasticity for all these models. Next we will derive the isochoric parts individually.

The isochoric Kirchhoff stress $\boldsymbol{\tau}_{\text{iso}}$ for Mooney–Rivlin model is transformed from Eq. (15):

$$\begin{aligned}\boldsymbol{\tau}_{\text{iso}} &= \mathbf{F}\mathbf{S}_{\text{iso}}\mathbf{F}^T \qquad \text{(A.6)}\\ &= \mathbf{F}J^{-2/3}\left[-\frac{1}{3}(\mu_1\bar{I}_1 + 2\mu_2\bar{I}_2)\overline{\mathbf{C}}^{-1} + (\mu_1 + \mu_2\bar{I}_1)\mathbf{I} - \mu_2\overline{\mathbf{C}}\right]\mathbf{F}^T,\\ &= -\frac{1}{3}(\mu_1\bar{I}_1 + 2\mu_2\bar{I}_2)\mathbf{I} - \mu_2\overline{\mathbf{B}}^2 + (\mu_1 + \mu_2\bar{I}_1)\overline{\mathbf{B}}\end{aligned}$$

where $\bar{\mathbf{B}}$ is the modified right Cauchy–Green tensor defined as $\overline{\mathbf{B}} = \overline{\mathbf{F}}\overline{\mathbf{F}}^T = \overline{\mathbf{C}}^T$, and the isochoric spatial tensor of elasticity $\mathbb{C}_{\text{iso}}$ is obtained from Eq. (25):

$$\begin{aligned}(c_{\text{iso}})_{ijkl} &= F_{iI}F_{jJ}F_{kK}F_{lL}(C_{\text{iso}})_{IJKL} \qquad \text{(A.7)}\\ &= 2\mu_2\left[\overline{\mathbf{B}}_{ij}\overline{\mathbf{B}}_{kl} - \frac{1}{2}(\overline{\mathbf{B}}_{ik}\overline{\mathbf{B}}_{jl} + \overline{\mathbf{B}}_{il}\overline{\mathbf{B}}_{jk})\right]\\ &- \frac{2}{3}(\mu_1 + 2\mu_2\bar{I}_1)(\overline{\mathbf{B}}_{ij}\delta_{kl} + \overline{\mathbf{B}}_{kl}\delta_{ij})\\ &+ \frac{4}{3}\mu_2(\overline{\mathbf{B}}^2_{ij}\delta_{kl} + \overline{\mathbf{B}}^2_{kl}\delta_{ij}) + \frac{2}{9}(\mu_1\bar{I}_1 + 4\mu_2\bar{I}_2)\delta_{ij}\delta_{kl}\\ &+ \frac{1}{3}(\mu_1\bar{I}_1 + 2\mu_2\bar{I}_2)(\delta_{ik}\delta_{jl} + \delta_{il}\delta_{jk})\,.\end{aligned}$$

Similarly, the isochoric stress $\boldsymbol{\tau}_{\text{iso}}$ and the isochoric spatial tensor of elasticity $\mathbb{C}_{\text{iso}}$ for Yeoh model are transformed from Eqs. (28) and (36):

$$\begin{aligned}\boldsymbol{\tau}_{\text{iso}} &= \mathbf{F}\mathbf{S}_{\text{iso}}\mathbf{F}^T = \mathbf{F}J^{-2/3}[2c_1 + 4c_2(\bar{I}_1 - 3) + 6c_3(\bar{I}_1 - 3)^2]\left(\mathbf{I} - \frac{1}{3}\bar{I}_1\overline{\mathbf{C}}^{-1}\right)\mathbf{F}^T, \qquad \text{(A.8)}\\ &= [2c_1 + 4c_2(\bar{I}_1 - 3) + 6c_3(\bar{I}_1 - 3)^2]\left(\overline{\mathbf{B}} - \frac{1}{3}\bar{I}_1\mathbf{I}\right),\end{aligned}$$

$$
\begin{aligned}
(c_{\text{iso}})_{ijkl} &= F_{iI}F_{jJ}F_{kK}F_{lL}(C_{\text{iso}})_{IJKL} \\
&= [8c_2 + 24c_3(\bar{I}_1 - 3)]\overline{\mathbf{B}}_{ij}\overline{\mathbf{B}}_{kl} \\
&- \left[\frac{4}{3}c_1 + c_2\left(\frac{16}{3}\bar{I}_1 - 8\right) + 12c_3(\bar{I}_1 - 1)(\bar{I}_1 - 3)\right](\overline{\mathbf{B}}_{ij}\delta_{kl} + \overline{\mathbf{B}}_{kl}\delta_{ij}) \\
&+ \left[\frac{4}{9}c_1\bar{I}_1 + c_2\left(\frac{16}{9}\bar{I}_1^2 - \frac{8}{3}\bar{I}_1\right) + 4c_3\bar{I}_1(\bar{I}_1 - 1)(\bar{I}_1 - 3)\right]\delta_{ij}\delta_{kl} \\
&+ \left[\frac{2}{3}c_1\bar{I}_1 + \frac{4}{3}c_2(\bar{I}_1 - 3)\bar{I}_1 + 2c_3(\bar{I}_1 - 3)^2\bar{I}_1\right](\delta_{ik}\delta_{jl} + \delta_{il}\delta_{jk}).
\end{aligned} \tag{A.9}
$$

For the HGO model, we will first derive the isotropic parts of the isochoric Kirchhoff stress and the isochoric spatial tensor of elasticity by setting $\mu_2$ to 0 in Eqs. (A.6) and (A.7), respectively:

$$
\boldsymbol{\tau}_{\text{isotropic}} = -\frac{1}{3}\mu_1\bar{I}_1\mathbf{I} + \mu_1\overline{\mathbf{B}}, \tag{A.10}
$$

$$
(c_{\text{isotropic}})_{ijkl} = -\frac{2}{3}\mu_1(\overline{\mathbf{B}}_{ij}\delta_{kl} + \overline{\mathbf{B}}_{kl}\delta_{ij}) + \frac{2}{9}\mu_1\bar{I}_1\delta_{ij}\delta_{kl} + \frac{1}{3}\mu_1\bar{I}_1(\delta_{ik}\delta_{jl} + \delta_{il}\delta_{jk}). \tag{A.11}
$$

Next we derive the anisotropic part of the isochoric Kirchhoff stress by substituting Eq. (49) into Eq. (A.1):

$$
\begin{aligned}
\boldsymbol{\tau}_{\text{aniso}} &= \mathbf{F}\mathbf{S}_{\text{aniso}}\mathbf{F}^T \\
&= \mathbf{F}2J^{-2/3}\left[\sum_{i=4,6}\frac{\partial\Psi_{\text{aniso}}}{\partial\bar{I}_i}\left(\mathbf{A}_{0i} - \frac{1}{3}\bar{I}_i\overline{\mathbf{C}}^{-1}\right)\right]\mathbf{F}^T \\
&= 2\sum_{i=4,6}\left[\frac{\partial\Psi_{\text{aniso}}}{\partial\bar{I}_i}\left(\overline{\mathbf{F}}\mathbf{A}_{0i}\overline{\mathbf{F}}^T - \frac{1}{3}\bar{I}_i\overline{\mathbf{F}\mathbf{C}}^{-1}\overline{\mathbf{F}}^T\right)\right] \\
&= 2\sum_{i=4,6}\left[\frac{\partial\Psi_{\text{aniso}}}{\partial\bar{I}_i}\bar{I}_i\left(\mathbf{A}_i - \frac{1}{3}\mathbf{I}\right)\right],
\end{aligned} \tag{A.12}
$$

where $\mathbf{A}_i$ is dyadic product of the deformed fiber vectors defined as $\mathbf{A}_i = \mathbf{a}_i \otimes \mathbf{a}_i$. The anisotropic part of the isochoric spatial tensor of elasticity is obtained by substituting Eq. (56) into Eq. (A.3):

$$(c_{\text{aniso}})_{ijkl} = F_{iI}F_{jJ}F_{kK}F_{lL}(C_{\text{aniso}})_{IJKL} \tag{A.13}$$
$$= \sum_{i=4,6}\left[4\bar{I}_i^2\frac{\partial^2\Psi_{\text{aniso}}}{\partial\bar{I}_i^2}\mathbf{A}_i\otimes\mathbf{A}_i - \frac{4}{3}\bar{I}_i\left(\bar{I}_i\frac{\partial^2\Psi_{\text{aniso}}}{\partial\bar{I}_i^2}+\frac{\partial\Psi_{\text{aniso}}}{\partial\bar{I}_i}\right)(\mathbf{A}_i\otimes\mathbf{I}+\mathbf{I}\otimes\mathbf{A}_i) + \frac{4}{9}\left(\bar{I}_i^2\frac{\partial^2\Psi_{\text{aniso}}}{\partial\bar{I}_i^2}+\bar{I}_i\frac{\partial\Psi_{\text{aniso}}}{\partial\bar{I}_i}\right)\mathbf{I}\otimes\mathbf{I}+\frac{4}{3}\bar{I}_i\frac{\partial\Psi_{\text{aniso}}}{\partial\bar{I}_i}\mathbb{I}\right].$$

Therefore, the isochoric Kirchhoff stress is obtained by adding up Eqs. (A.10) and (A.12), and the isochoric spatial tensor of elasticity is obtained by adding up Eqs. (A.11) and (A.13), respectively:

$$\boldsymbol{\tau}_{\text{iso}} = -\frac{1}{3}\mu_1\bar{I}_1\mathbf{I}+\mu_1\overline{\mathbf{B}}+2\sum_{i=4,6}\left[\frac{\partial\Psi_{\text{aniso}}}{\partial\bar{I}_i}\bar{I}_i\left(\mathbf{A}_i-\frac{1}{3}\mathbf{I}\right)\right]. \tag{A.14}$$

$$(c_{\text{iso}})_{ijkl} = -\frac{2}{3}\mu_1(\overline{\mathbf{B}}_{ij}\delta_{kl}+\overline{\mathbf{B}}_{kl}\delta_{ij})+\frac{2}{9}\mu_1\bar{I}_1\delta_{ij}\delta_{kl}+\frac{1}{3}\mu_1\bar{I}_1(\delta_{ik}\delta_{jl}+\delta_{il}\delta_{jk}) \tag{A.15}$$
$$+\sum_{i=4,6}\left[4\bar{I}_i^2\frac{\partial^2\Psi_{\text{aniso}}}{\partial\bar{I}_i^2}\mathbf{A}_i\otimes\mathbf{A}_i-\frac{4}{3}\bar{I}_i \times\left(\bar{I}_i\frac{\partial^2\Psi_{\text{aniso}}}{\partial\bar{I}_i^2}+\frac{\partial\Psi_{\text{aniso}}}{\partial\bar{I}_i}\right)(\mathbf{A}_i\otimes\mathbf{I}+\mathbf{I}\otimes\mathbf{A}_i) + \frac{4}{9}\left(\bar{I}_i^2\frac{\partial^2\Psi_{\text{aniso}}}{\partial\bar{I}_i^2}-\bar{I}_i\frac{\partial\Psi_{\text{aniso}}}{\partial\bar{I}_i}\right)\mathbf{I}\otimes\mathbf{I}+\frac{4}{3}\bar{I}_i\frac{\partial\Psi_{\text{aniso}}}{\partial\bar{I}_i}\mathbb{I}\right].$$

To summarize, Tables 1 and 2 list the equation numbers of the derived stress and elasticity tensors for Mooney–Rivlin, Yeoh and HGO models in the reference configuration and the current configuration, respectively.

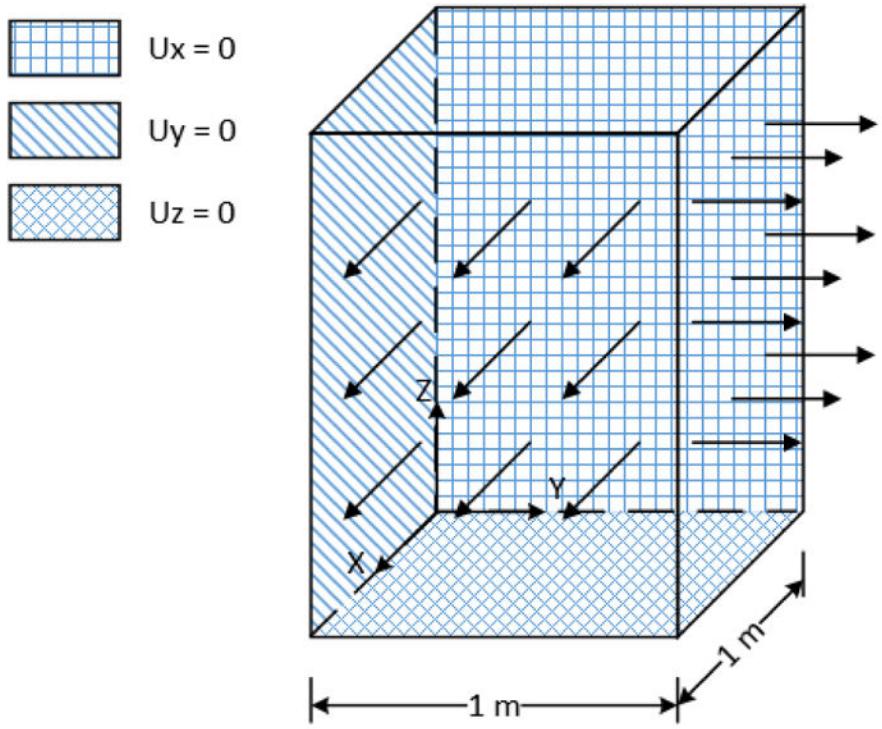


**Fig. 1.**
Model setup for biaxial tension test.

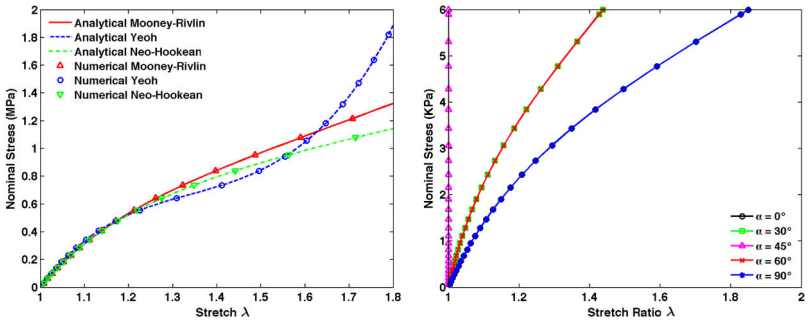


(a) Isotropic models (b) HGO model

**Fig. 2.**
Relationship of nominal stress to stretch in biaxial tension test.

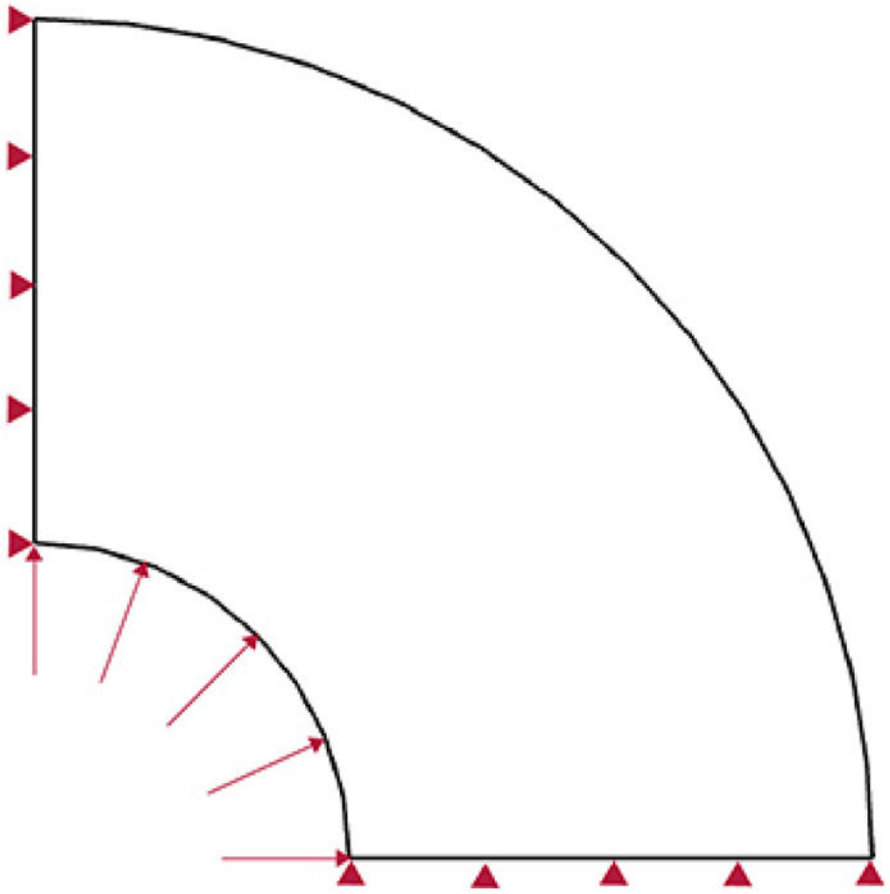

**Fig. 3.**
Cross-section of the vessel.

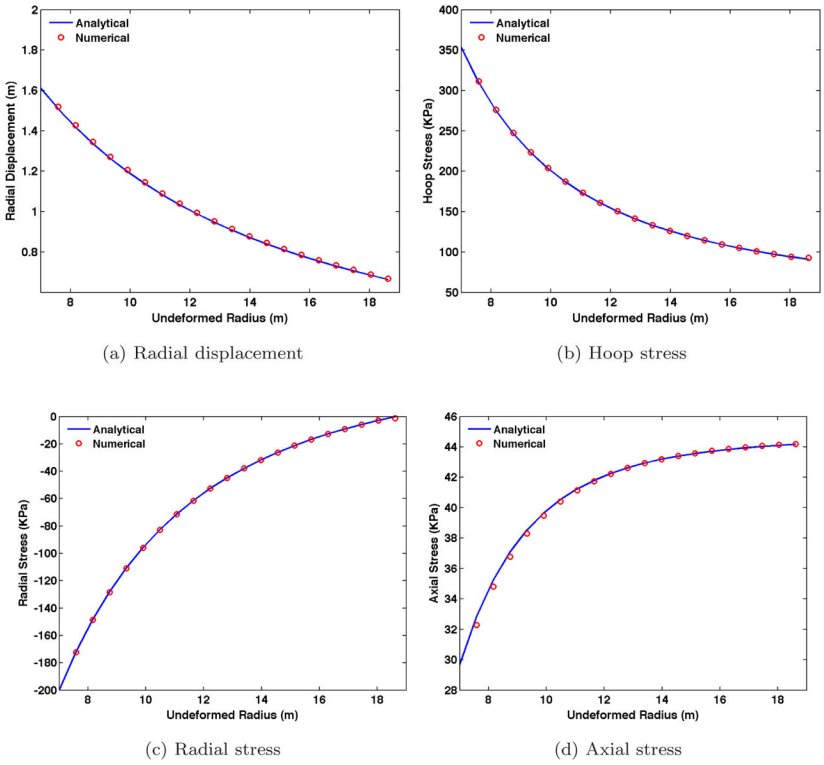


**Fig. 4.**
Vessel expansion under internal pressure of $P_i$ = 200KPa.

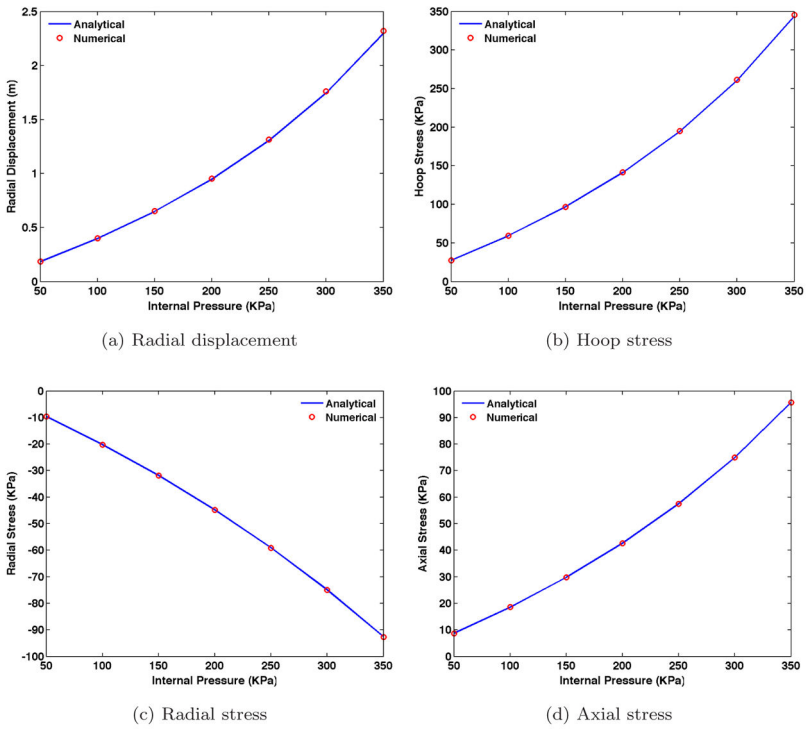


(a) Radial displacement (b) Hoop stress

(c) Radial stress (d) Axial stress

**Fig. 5.**
Vessel expansion under different pressure with Mooney–Rivlin model.

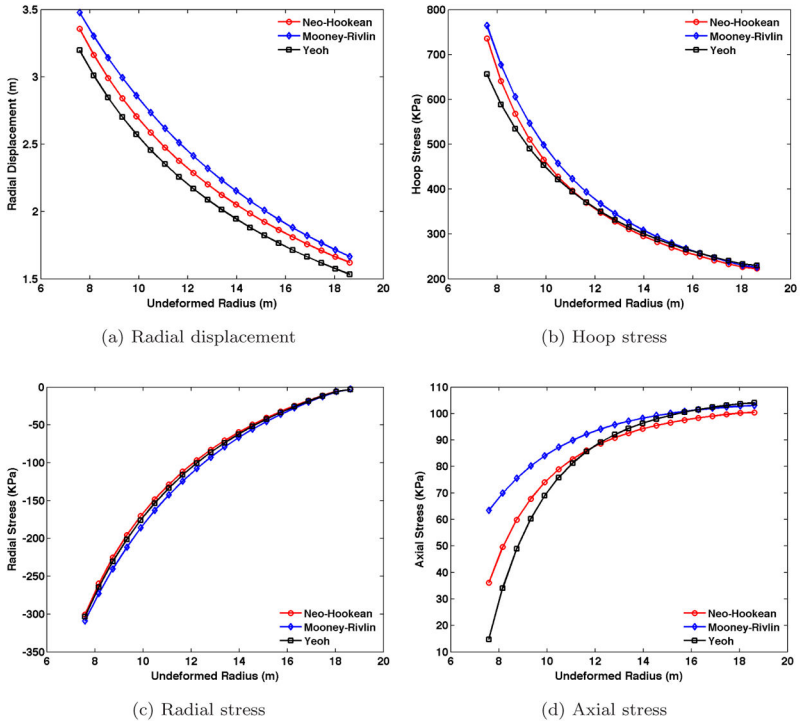


**Fig. 6.**

Vessel expansion under inner pressure of $P_i$ = 350KPa using different hyperelastic models.

**Table 1**

Equations in the reference configuration.

| | Stress tensor | | Elasticity tensor | |
|---|---|---|---|---|
| **Model** | **Isochoric** | **Volumetric** | **Isochoric** | **Volumetric** |
| Mooney–Rivlin | 15 | | 25 | |
| Yeoh | 28 | 13a (mixed) or 13b (disp.) | 36 | 17a (mixed) or 17b (disp.) |
| HGO | 50 | | 57 | |

**Table 2**

Equations in the current configuration.

| | Stress tensor | | Elasticity tensor | |
|---|---|---|---|---|
| **Model** | **Isochoric** | **Volumetric** | **Isochoric** | **Volumetric** |
| Mooney–Rivlin | A.6 | | A.7 | |
| Yeoh | A.8 | A.4b (mixed) or A.4c (disp.) | A.8 | A.5b (mixed) or A.5c (disp.) |
| HGO | A.14 | | A.15 | |

**Table 3**

Material parameters of the isotropic models.

| Neo–Hookean | Mooney–Rivlin | Yeoh |
|---|---|---|
| $\mu_1 = 0.595522$ MPa | $\mu_1 = 0.595522$ MPa | $c_1 = 0.358756$ MPa |
| | $\mu_2 = 0.050381$ MPa | $c_2 = -0.0508009$ MPa |
| | | $c_3 = 0.0142132$ MPa |
| For all models, $\kappa = 1 \times 10^5$ MPa | | |